Supplementary Information
for

Monoradical-Containing Four-Coordinate Co(III) Complexes: Homolytic S-S, Se-Se Bond Cleavage and Catalytic Isocyanate to Urea Conversion Under Sunlight

Ganesh Chandra Paul,[a†] Samir Ghorai[a†] and Chandan Mukherjee[a]*

***Corresponding address:**

Dr. Chandan Mukherjee, Department of Chemistry, Indian Institute of Technology Guwahati, Guwahati, 781039, Assam, India

Email: cmukherjee@iitg.ernet.in

Phone No. +91-361-258-2327

Fax: +91-361-258-2349

Contents	**Page**
Synthesis of $\mathbf{H_2L^{AP(Me)}}$ and $\mathbf{H_2L^{AP(Ph)}}$	S3
Synthesis of complexes **1**, **1a**, **2**, **2a** and **2b**	S4-S5
General method for catalysis reaction	S6
FT-IR spectrum of $\mathbf{H_2L^{AP(Ph)}}$	S7
ESI-MS (+ve mode) mass spectra for ligand $\mathbf{H_2L^{AP(Ph)}}$	S7
^{1}H-NMR spectrum of $\mathbf{H_2L^{AP(Ph)}}$	S8
^{13}C NMR spectrum of $\mathbf{H_2L^{AP(Ph)}}$	S8
FT-IR spectrum of complexes **1**, **1a** and **1b**	S9-S10
FT-IR spectrum of complexes **2**, **2a**, **2b** and **2c**	S10- S12
ESI-MS (+ve mode) mass spectra for complex **1**	S12
ESI-MS (+ve mode) mass spectra for complex **1a** and complex **1b**	S13
ESI-MS (+ve mode) mass spectra for complex **2** and complex **2a**	S14
ESI-MS (+ve mode) mass spectra for complex **2b**	S15
^{1}H-NMR spectrum of complex **1a**	S15
^{1}H-NMR spectrum of complex **2a** and complex **2b**	S16
ORTEP diagram of complex **1b** and **2c**	S17
X-band EPR spectrum of complex **1** and complex **2**	S18
UV-Vis/NIR spectrum of complex **1**	S18
UV-Vis/NIR spectrum of complex **1a** and complex **1b**	S19
UV-Vis/NIR spectrum of complex **2** and complex **2a**	S20
UV-Vis/NIR spectrum of complex **2b** and complex **2c**	S21
Change in UV-Vis/NIR spectrum of **1a** upon exposure to sunlight and X-band EPR spectrum of irradiated solution of **1a** in CH_2Cl_2	S22
Change in UV-Vis/NIR spectrum of **2a** upon exposure to sunlight and X-band EPR spectrum of irradiated solution of **2a** in CH_2Cl_2	S22
Change in UV-Vis/NIR spectrum of **2b** upon exposure to sunlight and X-band EPR spectrum of irradiated solution of **2b** in CH_2Cl_2	S23
Change in X-band EPR spectrum of complex **1** and **2** with Ph_2S_2 and Ph_2Se_2 in CH_2Cl_2 solution	S23
GC-MS spectrum during catalysis reaction	S24
^{1}H-NMR spectrum of **4a** and **4b**	S25
ESI-MS (+ve mode) mass spectra for **4a** and **4b**	S26
Selected bond distances (Å) and bond angles (°) of complex **1**	S27
Selected bond distances (Å) and bond angles (°) of complex **1a**	S27
Selected bond distances (Å) and bond angles (°) of complex **1b**	S28
Selected bond distances (Å) and bond angles (°) of complex **2a**	S28
Selected bond distances (Å) and bond angles (°) of complex **2b** (at 100 K).	S29
Selected bond distances (Å) and bond angles (°) of complex **2c**	S30
Crystallographic parameters and refinement data for complex **1**	S31
Crystallographic parameters and refinement data for complex **1a**	S32
Crystallographic parameters and refinement data for complex **1b**	S33
Crystallographic parameters and refinement data for complex **2a**	S34
Crystallographic parameters and refinement data for complex **2b** (at 100 K).	S35
Crystallographic parameters and refinement data for complex **2c**.	S36
References	S37

Materials: All the chemicals and solvents were obtained from commercial sources and were used as supplied, unless noted otherwise. 3,5–di–*tert*–butylcatechol, *o*–toluidine, 2–aminobiphenyl, diphenyl diselenide were purchased from Sigma–Aldrich. Diphenyl disulfide was synthesized according to the previous report.[1] Solvents were obtained from Merck (India). Mass spectra were measured in HPLC grade acetonitrile solution.

Physical methods: X-ray crystallographic data were collected using Super Nova, Single source at offset, Eos diffractometer. The data refinement and cell reductions were carried out by CrysAlisPro.[2] Structures were solved by direct methods using SHELXS–97 and refined by the full matrix least squares method using SHELXL–97.[3] All the non–hydrogen atoms were refined anisotropically. IR spectra were recorded on a Perkin Elmer Instrument at normal temperature with KBr pellet by grinding the sample with KBr (IR Grade). ^{1}H–, and ^{13}C–NMR spectra of the ligand were recorded either in Varian 400 or in BRUKER 600 MHz NMR machines. UV–vis/NIR spectra, and spectroelectrochemical data were recorded on a Perkin Elmer, Lamda 750, UV/VIS/NIR spectrometer by preparing a known concentration of the samples in HPLC Grade CH_2Cl_2 at room temperature (25 °C) using a cuvette of 1 cm width.

Synthesis of $H_2L^{AP(Me)}$ [$C_{21}H_{29}NO$]: Reported previously.[4]

Synthesis of $H_2L^{AP(Ph)}$ [$C_{26}H_{31}NO$]: To a stirred solution of 2–animobiphenyl (0.848 g, 5.01 mmol) in hexane (20 mL), 3,5–di–*tert*–bulyl catechol (1.117 g, 5.02 mmol) and Et_3N (0.05 ml) were added sequentially at room temperature (25 °C) under air. A reddish brown homogeneous solution was obtained on refluxing the reaction mixture for 2 days. Then the solution mixture was cooled to room temperature and stirred for another 2 days. All the solvent was evaporated under vacuum and product was purified by column chromatography using hexane:ethyl acetate (98:2) as the eluent to give $H_2L^{AP(Ph)}$. Yield: 1.65 g (88%). FTIR Spectra (KBr pellet cm^{-1}): 3538.85, 3427.06, 3360.01, 3056.49, 2995.96, 2961.22, 2903.57, 2865.07, 1594.53, 1580.22, 1503.89, 1484.58, 1436.16, 1419.48, 1359.73, 1308.55, 1264.53, 1222.24, 1199.47, 1007.96, 764.74, 756.23, 743.09, 700.67, 608.47. ^{1}H NMR(600 MHz, $CDCl_3$) δ (ppm): 7.55 (d, J = 7.1 Hz, 2H), 7.51 (t, J = 7.0 Hz, 2H), 7.41 (t, J = 6.9 Hz, 1H), 7.23-7.22 (d, 2H), 7.18 (t, J = 7.6 Hz, 1H), 6.98 (s 1H), 6.93 (t, J = 7.2 Hz, 1H), 6.56 (d, J = 8.0 Hz, 1H), 6.40 (s, 1H), 5.22 (s, 1H) ,1.44 (s, 9H), 1.26 (s, 9H). ^{13}C NMR (150 MHz, $CDCl_3$): δ 29.7, 31.8, 34.6, 35.2, 114.5, 119.8, 121.8, 122.2, 127.8, 128.0, 128.9, 129.4, 129.6, 130.6, 135.4, 139.1, 142.4, 144.0, 149.7 ppm. ESI-MS (+) m/z for $[C_{26}H_{31}NO+H]^+$: Calcd, 374.24; found, 374.24.

Synthesis of $[C_{42}H_{54}CoN_2O_2]$; $[CoL^{AP(Me)}L^{ISQ(Me)}]$ (1): Ligand $H_2L^{AP(Me)}$ (0.312 g, 1.0 mmol) was taken in acetonitrile (10 mL). $Co(ClO_4)_2{\bullet}6H_2O$ (0.365 g, 1.0 mmol) and Et_3N (0.2 mL) were added sequentially to the solution and allowed to stir for 1 hour under air. The resulting reaction mixture was filtered and washed with acetonitrile to obtain green solid. X–ray quality single crystals were obtained by slow evaporation of a diethyl ether:acetonitrile (5:1) solution of the solid. Yield: 0.282 g, 83%. FT–IR (KBr pellet, cm^{-1}): 2954, 2901, 2862, 1537, 1478, 1458, 1358, 1301, 1258, 1181, 1146, 1107, 1026, 912, 896, 856, 754, 738, 658, 517. ESI–MS (CH_3CN) *m/z* for $[C_{42}H_{54}CoN_2O_2]^+$: Calcd, 677.35; Found, 677.44. Anal. Calcd for $C_{42}H_{54}CoN_2O_2$: C, 74.41; H, 8.03; N, 4.13 %. Found: C, 74.34; H, 7.89; N, 4.51 %.

Synthesis of $[C_{48}H_{59}CoN_2O_2S]$; $[Co\{L^{ISQ(Me)}\}_2SPh]$ (1a): Diphenyl disulfide (0.066 g, 0.3 mmol) was added to a stirring solution of $[CoL^{AP(Me)}L^{ISQ(Me)}]$ (0.138 g, 0.2 mmol) in diethyl ether (30 mL). Acetonitrile (10 mL) was added to the resulting reaction mixture and kept it in a dark place for slow solvent evaporation. Crystalline solid of $[Co\{(L^{Me})^{ISQ}\}_2SPh]$ was isolated within two days. The crystal was suitable for single crystal X–ray diffraction measurement. Yield: 0.142 g, 90%. FTIR (KBr pellet, cm^{-1}): 2960, 2905, 2867, 1598, 1525, 1481, 1459, 1406, 1362, 1300, 1264, 1230, 1204, 1175, 1144, 1113, 1103, 1025, 1000, 914, 860, 755, 742, 724, 690, 666. ESI-MS (+) m/z for $[C_{48}H_{59}CoN_2O_2S]^+$: Calcd, 786.36; found, 786.36. Anal. Calcd for $C_{48}H_{59}CoN_2O_2S$: C, 73.25; H, 7.56; N, 3.56 %. Found: C, 73.46; H, 7.38; N, 3.44 %.

Synthesis of $[C_{52}H_{58}CoN_2O_2]$; $[CoL^{AP(Ph)}L^{ISQ(Ph)}]$ (2): To a stirred solution of ligand $H_2L^{AP(Ph)}$ (0.189 g, 0.5 mmol) in acetonitrile (10 mL), $Co(ClO_4)_2{\bullet}6H_2O$ (0.187 g, 0.5 mmol) and Et_3N (0.1 mL) were added sequentially at room temperature under air. The solution was then stirred at room temperature for an hour. The resulted precipitate was filtered and washed with excess acetonitrile (10 mL). Unfortunately, all attempts to grow single crystals of $[Co(L^{Ph})^{AP}(L^{Ph})^{ISQ}]$ were unsuccessful. Yield: 0.104 g, 52%. FT–IR (KBr pellet, cm^{-1}): 3054, 2953, 2902, 2863, 1577, 1536, 1474, 1358, 1302, 1266, 1185, 1140, 1106, 1026, 912, 896, 855, 746, 697, 660, 510. ESI-MS (+) m/z for $[C_{52}H_{58}CoN_2O_2]^+$: Calcd, 801.38; found, 801.38. Anal. Calcd for $C_{52}H_{58}CoN_2O_2$: C, 77.87; H, 7.29; N, 3.49 %. Found: C, 78.10; H, 7.28; N, 3.16 %.

Synthesis of [$C_{58}H_{63}CoN_2O_2S$]; [$Co\{L^{ISQ(Ph)}\}_2SPh$] (2a): Ligand $H_2L^{AP(Ph)}$ (0.187 g, 0.50 mmol) was dissolved in acetonitrile (10 mL), $Co(ClO_4)_2 \bullet 6H_2O$ (0.092 g, 0.25 mmol) was added to the solution at room temperature. During stirring the colour of the solution gradually turned to deep blue. The solution was then treated with triethylamine (0.1 mL). After 15 min, diphenyl disulfide (0.110 g, 0.5 mmol) was added to the blue solution. The solution was further stirred for 2.5 h. A blue colour precipitate was formed, which was isolated by filtration and washed thoroughly with acetonitrile (10 mL). X–ray quality single crystals were grown from a solvent mixture of diethyl ether and acetonitrile (4:1) in a dark place using solvent evaporation technique. Yield: 0.107 g, 47%. FTIR (KBr pellet, cm^{-1}): 3052, 2956, 2903, 2866, 1591, 1527, 1472, 1432, 1392, 1361, 1331, 1298, 1268, 1243, 1202, 1175, 1104, 1025, 747, 698. ESI–MS (+) m/z for $[C_{58}H_{63}CoN_2O_2S]^+$: Calcd, 910.39; Found 910.39. Anal. Calcd for $C_{58}H_{63}CoN_2O_2S$: C, 76.45; H, 6.97; N, 3.08 %. Found: C, 77.18; H, 7.12; N, 3.17%.

Synthesis of [$C_{58}H_{63}CoN_2O_2Se$]; [$Co\{L^{ISQ(Ph)}\}_2SePh$] (2b): To a stirred solution of ligand $H_2L^{AP(Ph)}$ (0.187 g, 0.50 mmol)) in acetonitrile (10 mL), $Co(ClO_4)_2 \bullet 6H_2O$ (0.092 g, 0.25 mmol) and triethylamine (0.1 mL) were added, sequentially. The resulted solution was stirred for 15 min and then diphenyl diselenide (0.110 g, 0.5 mmol) was added to the solution. The blue solution was further stirred for 2.5 h. A deep blue colour precipitate was formed during the stirring. The solid was filtered and washed with acetonitrile (15 mL). X–ray quality single crystals were obtained by slow evaporation of diethyl ether:acetonitrile (4:1) solution of the complex at room temperature in a dark place. Yield: 0.080 g, 33%. FTIR (KBr pellet, cm^{-1}): 3056, 2961, 2903, 2863, 1525, 1462, 1431, 1361, 1297, 1261, 1202, 1175, 1099, 1026, 802, 784, 735, 696. ESI–MS (+) m/z for $[C_{58}H_{63}CoN_2O_2Se]^+$: Calcd, 958.34; Found 958.33. Anal. Calcd for $C_{58}H_{63}CoN_2O_2Se$: C, 72.63; H, 6.63; N, 2.92 %. Found: C, 72.87; H, 6.63; N, 2.95 %.

General method for the catalysis: A pressure tube was initially evacuated and then filled with argon. The process was repeated thrice. After that catalyst (**1**/**2**/**2a**) and dry dichloromethane (5.0 mL) were added. The solution was stirred for a few minutes and then to the catalyst solution isocyanate substrate was added by a syringe. The septum was then replaced by a Teflon screw cap under the argon flow. The reaction solution was then stirred under sunlight for 6 h, during which product was separated as white solid. The solid was collected by filtration and washed with dichloromethane.

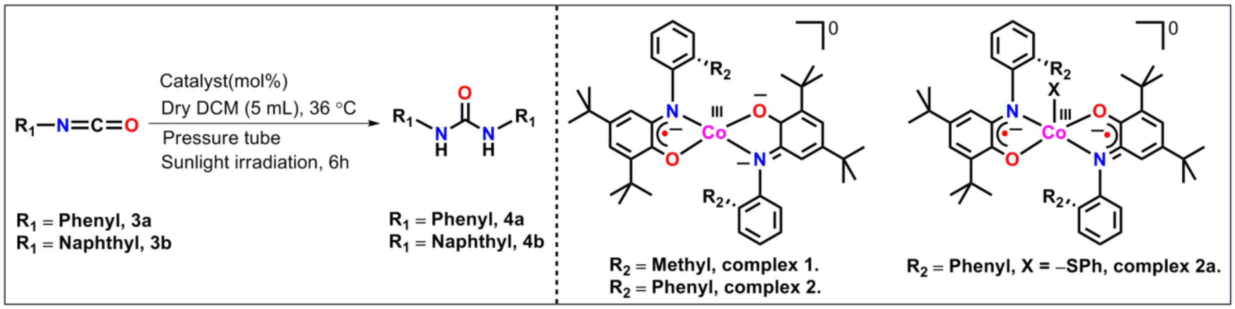

Scheme S1. Reaction scheme for the catalysis.

Table S1. Catalysis at variable condition.

Entry	**Substrate**	**Product**	**Cat. Used (mol %)**			**Yield (%)**		
			1	**2**	**2a**	**1**	**2**	**2a**
1	**3a**	**4a**	2.5	2.5	2.5	72	78	76
2	**3a**	NR	0	0	0	0	0	0
3	**3b**	**4b**	2.5	2.5	2.5	80	86	82
4	**3b**	NR	0	0	0	0	0	0
5	**3a**	**4a**	–	1.0	–	–	72	–
6	**3a**	**4a**	–	0.1	–	–	48	–

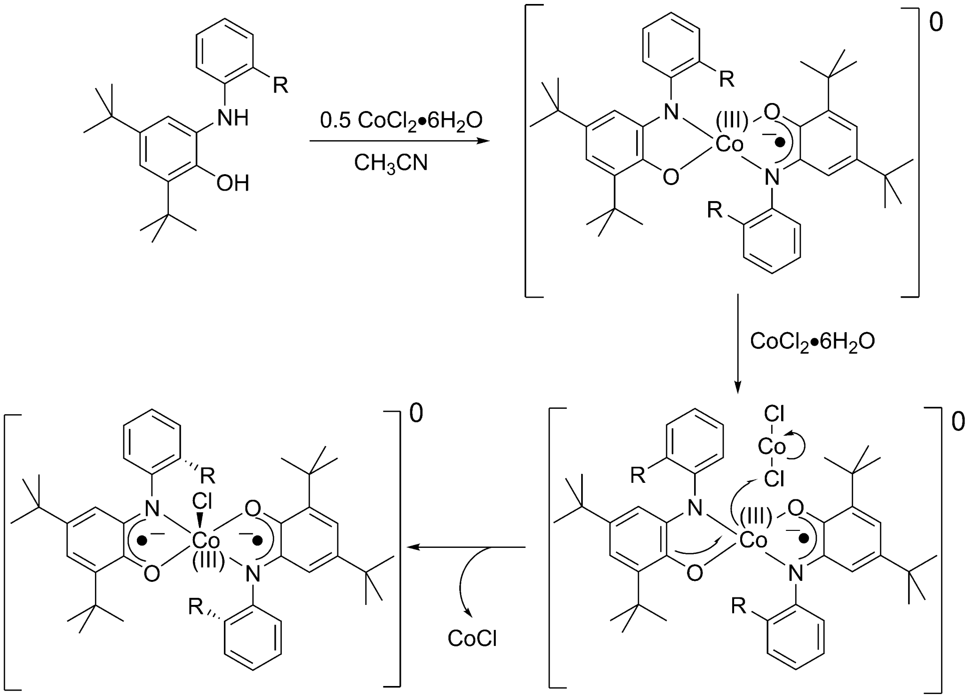

Scheme S2. Proposed mechanism for the formation of five-coordinate chloride-bound complexes.

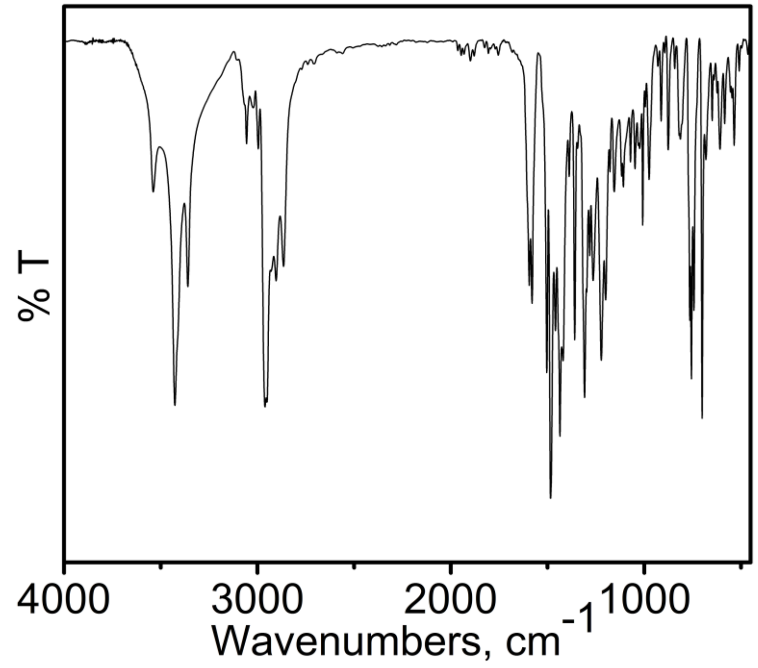

Figure S1. FT-IR spectrum of **$H_2L^{AP(Ph)}$**.

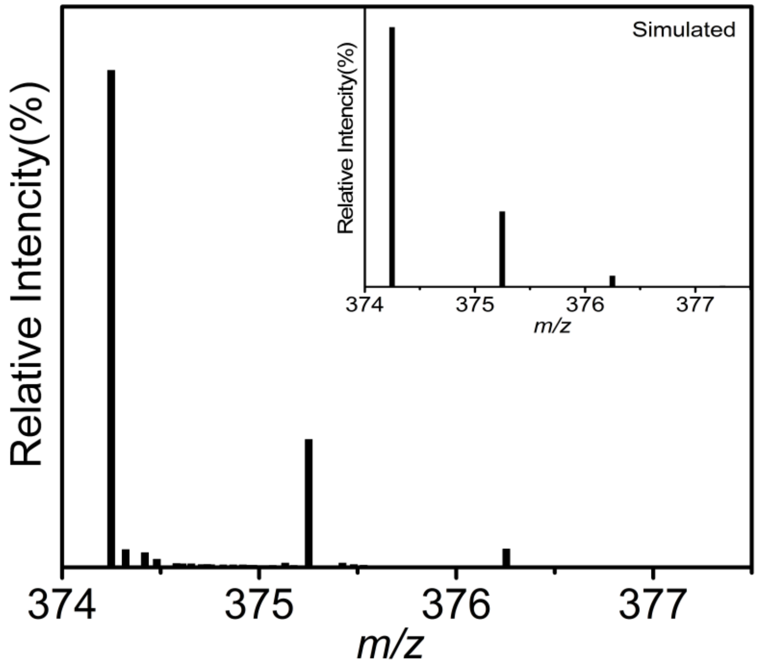

Figure S2. Experimental and simulated mass spectra for **$H_2L^{AP(Ph)}$** $[C_{26}H_{31}NO+H]^+$ have been shown.

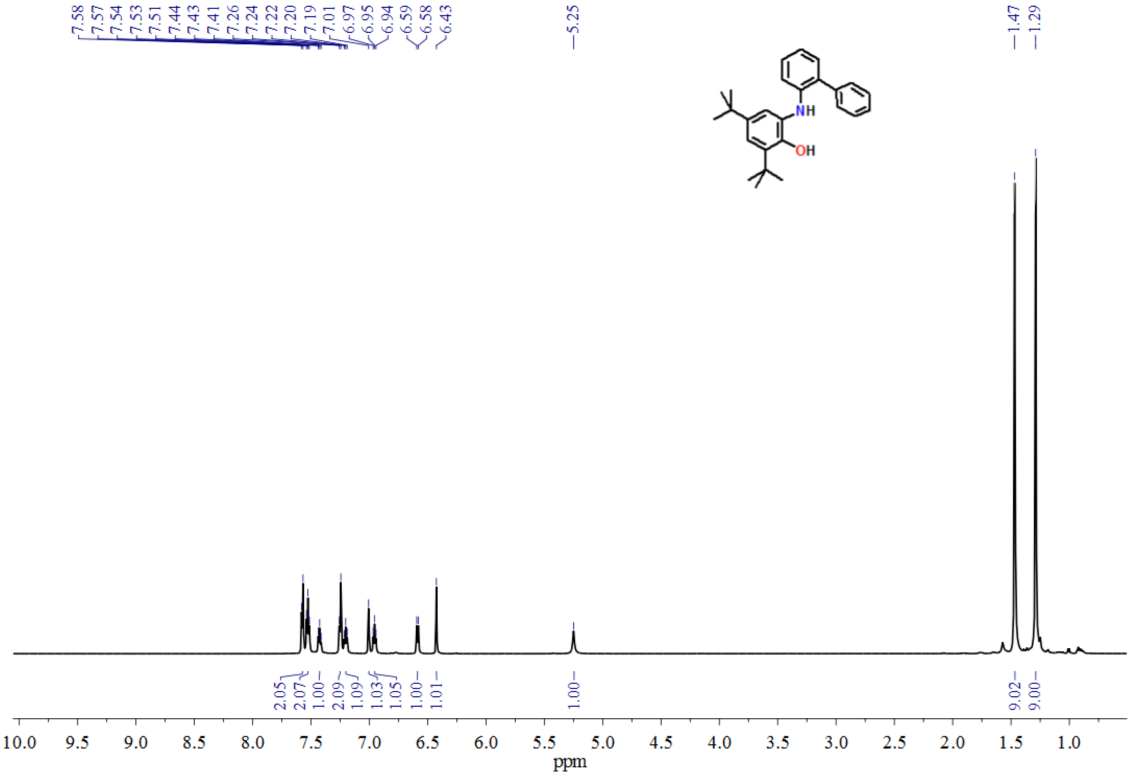

Figure S3. ^{1}H-NMR spectrum of $\mathbf{H_2L^{AP(Ph)}}$ (in $CDCl_3$).

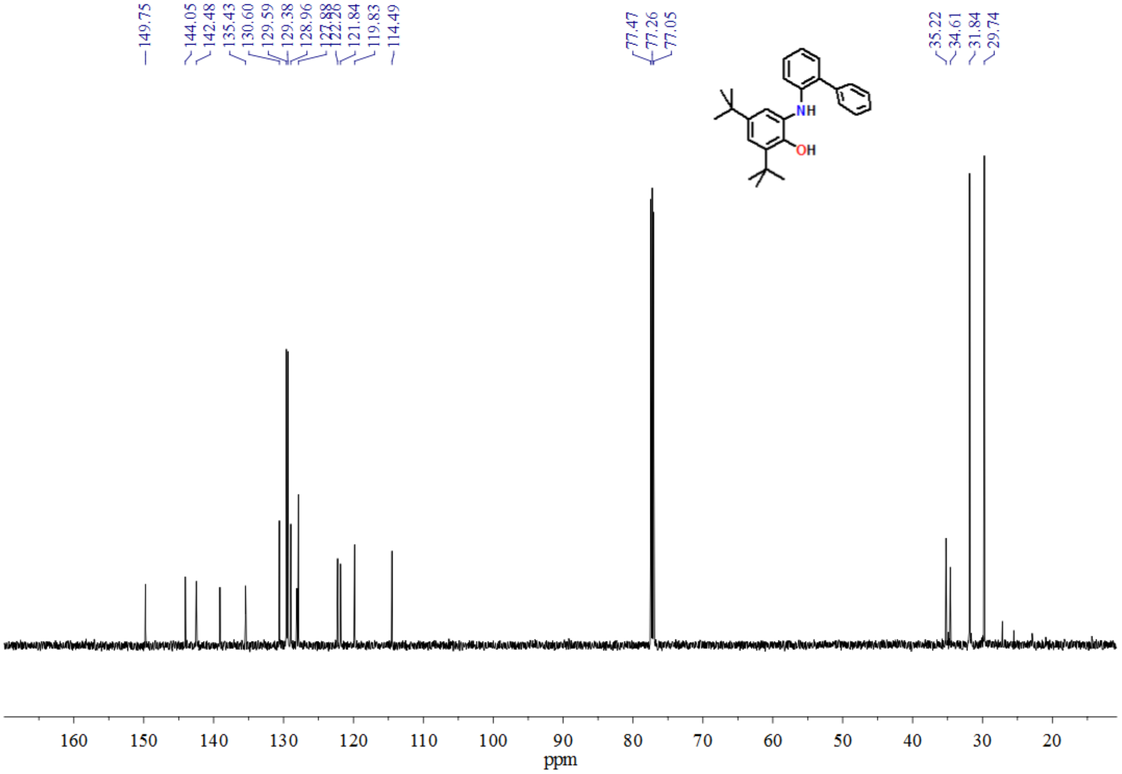

Figure S4. ^{13}C-NMR spectrum of $\mathbf{H_2L^{AP(Ph)}}$ (in $CDCl_3$).

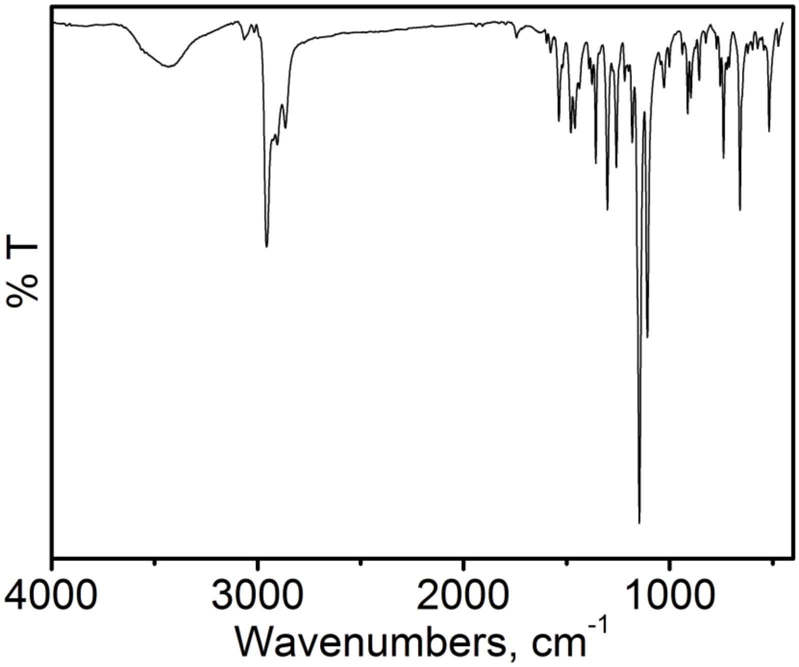

Figure S5. FT-IR spectrum of complex **1**.

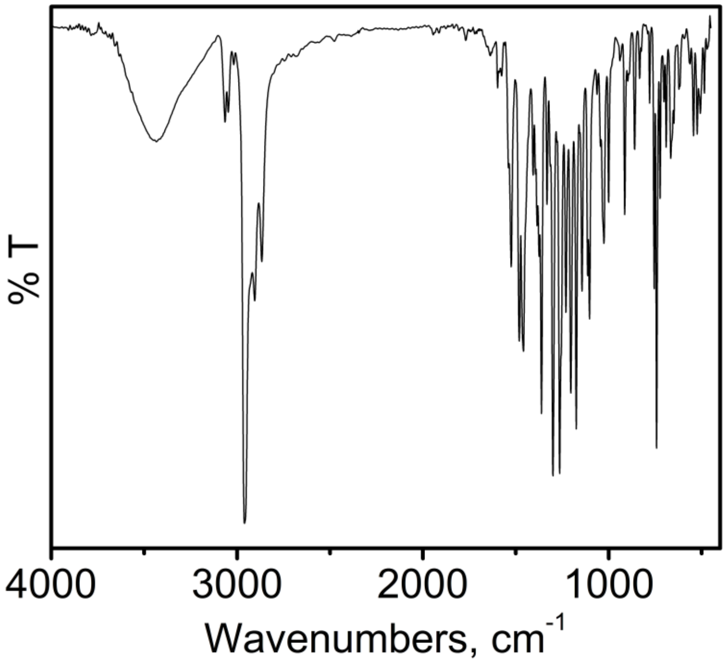

Figure S6. FT-IR spectrum of complex **1a**.

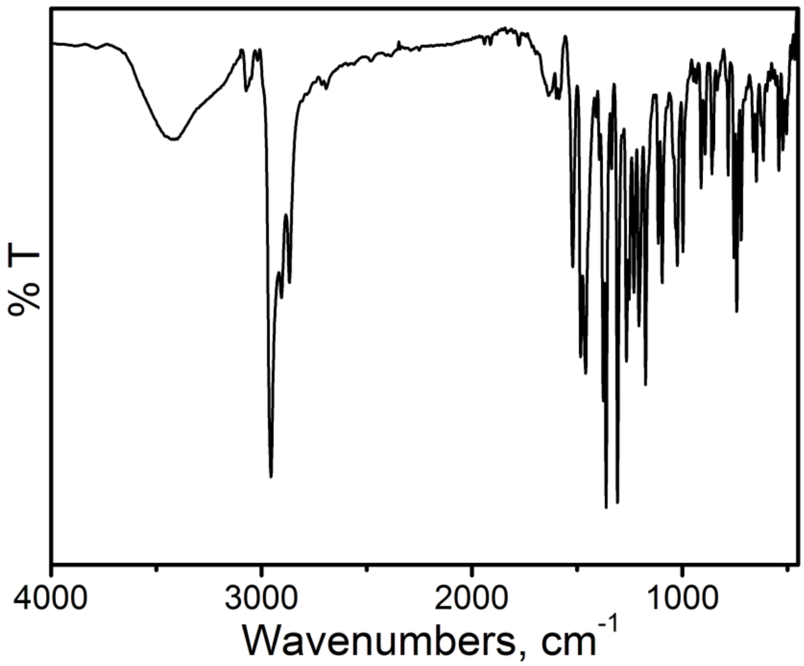

Figure S7. FT-IR spectrum of complex **1b**.

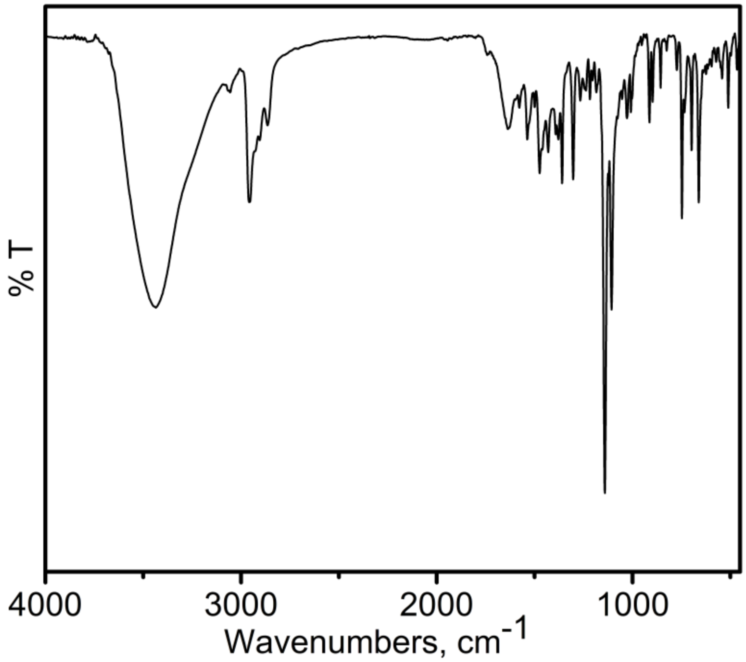

Figure S8. FT-IR spectrum of complex **2**.

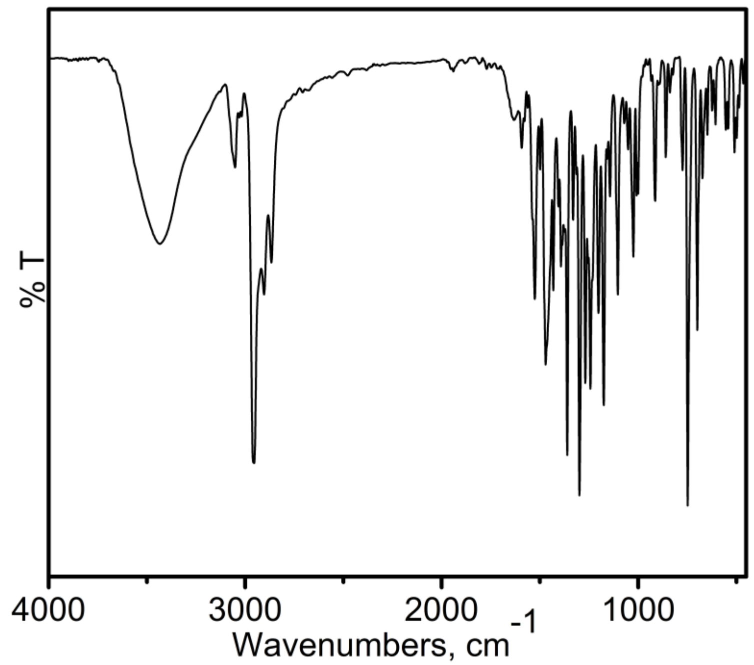

Figure S9. FT-IR spectrum of complex **2a**.

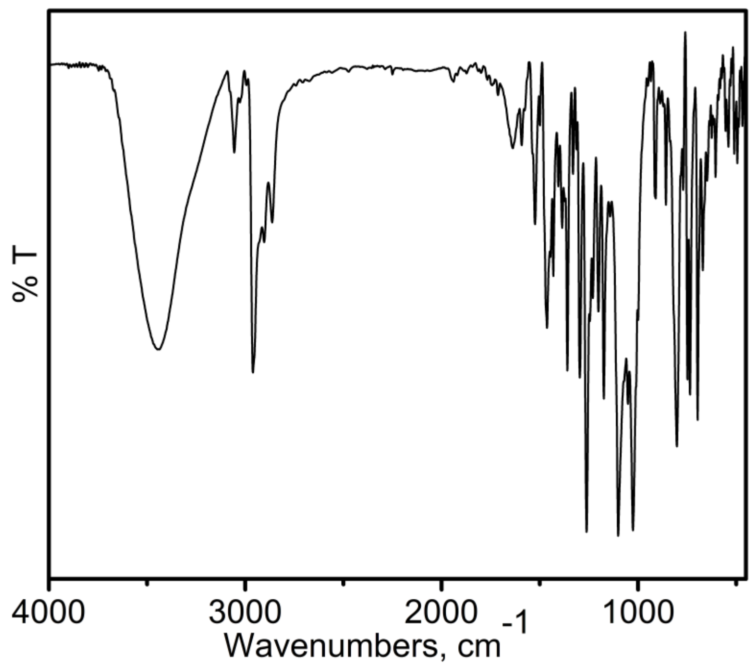

Figure S10. FT-IR spectrum of complex **2b**.

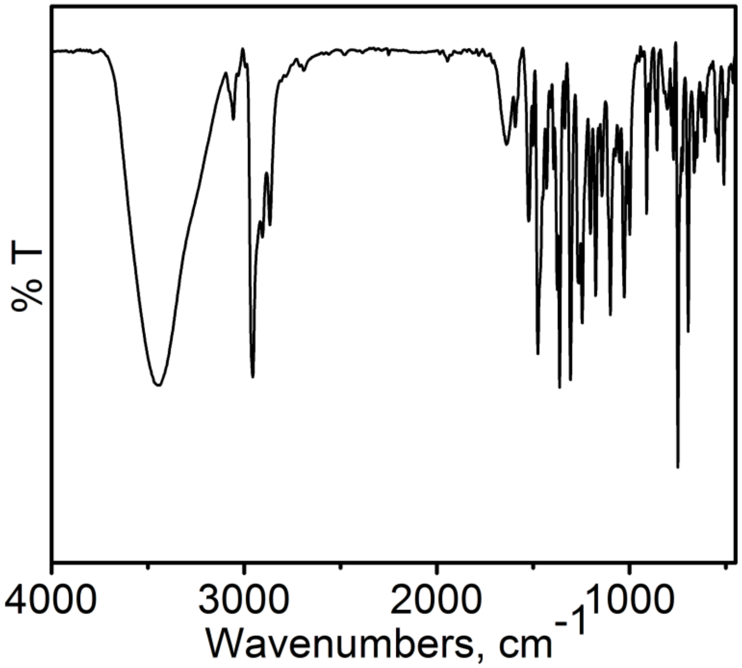

Figure S11. FT-IR spectrum of complex **2c**.

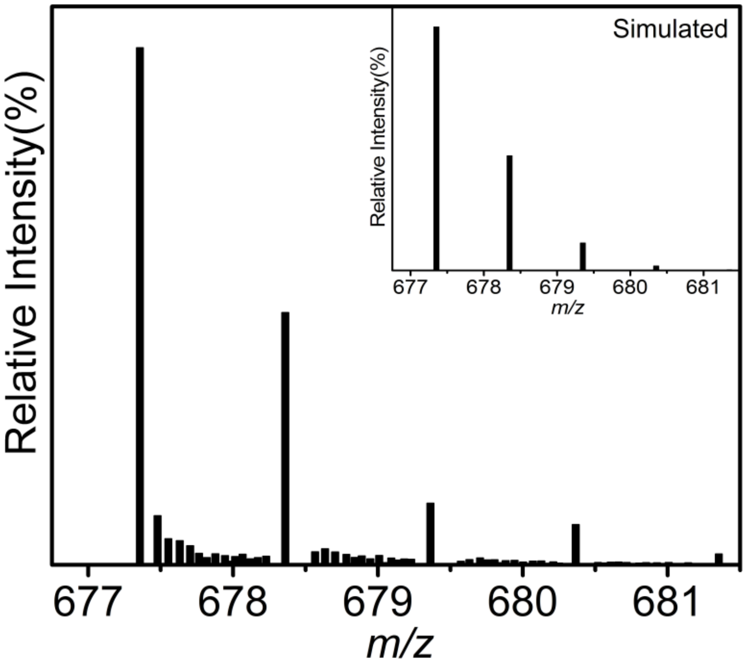

Figure S12. Experimental and simulated mass spectra for complex **1** $[C_{42}H_{54}CoN_2O_2]^+$ have been shown.

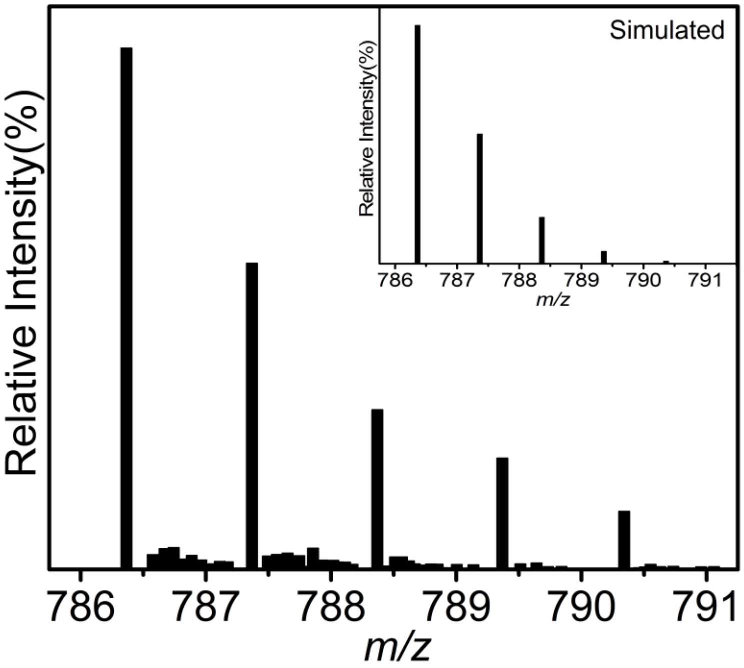

Figure S13. Experimental and simulated mass spectra for complex **1a** $[C_{48}H_{59}CoN_2O_2S]^+$ have been shown.

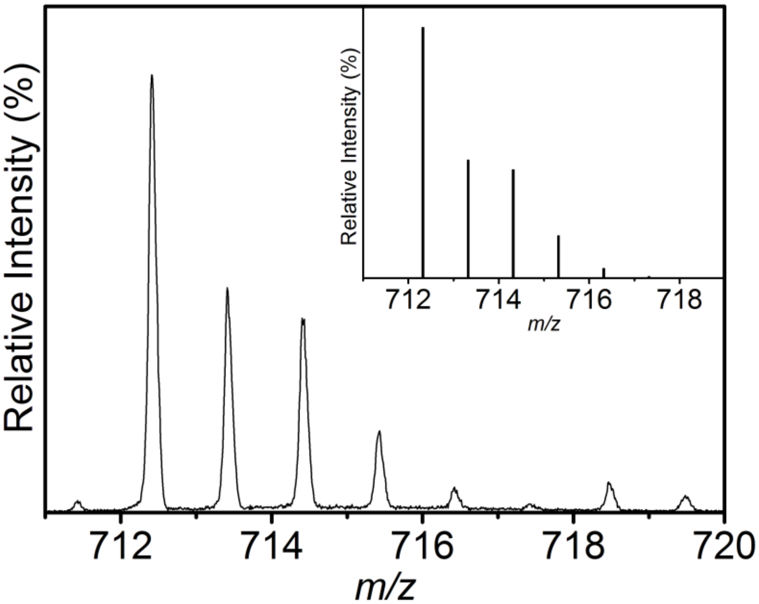

Figure S14. Experimental and simulated mass spectra for complex **1b** $[C_{42}H_{54}ClCoN_2O_2]^+$ have been shown.

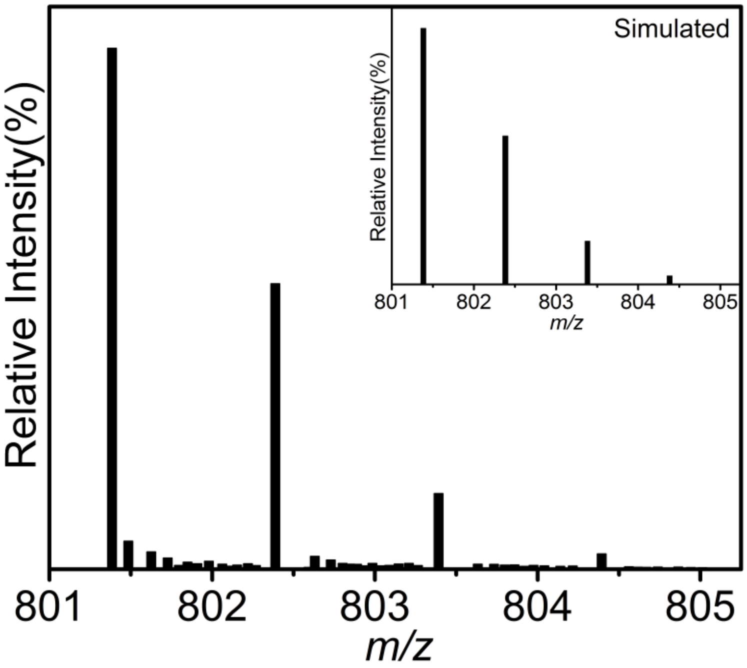

Figure S15. Experimental and simulated mass spectra for complex **2** $[C_{52}H_{58}CoN_2O_2]^+$ have been shown.

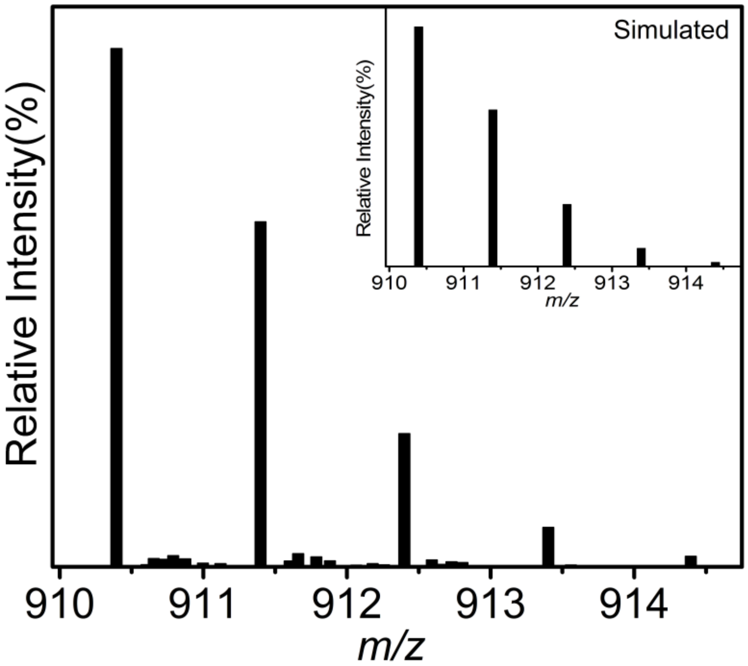

Figure S16. Experimental and simulated mass spectra for complex **2a** $[C_{58}H_{63}CoN_2O_2S]^+$ have been shown.

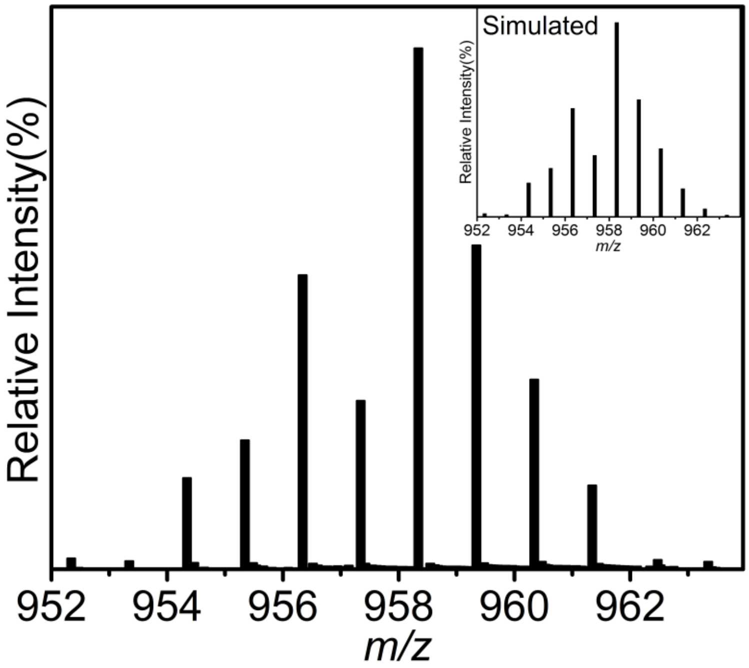

Figure S17. Experimental and simulated mass spectra for complex **2b** $[C_{58}H_{63}CoN_2O_2Se]^+$ have been shown.

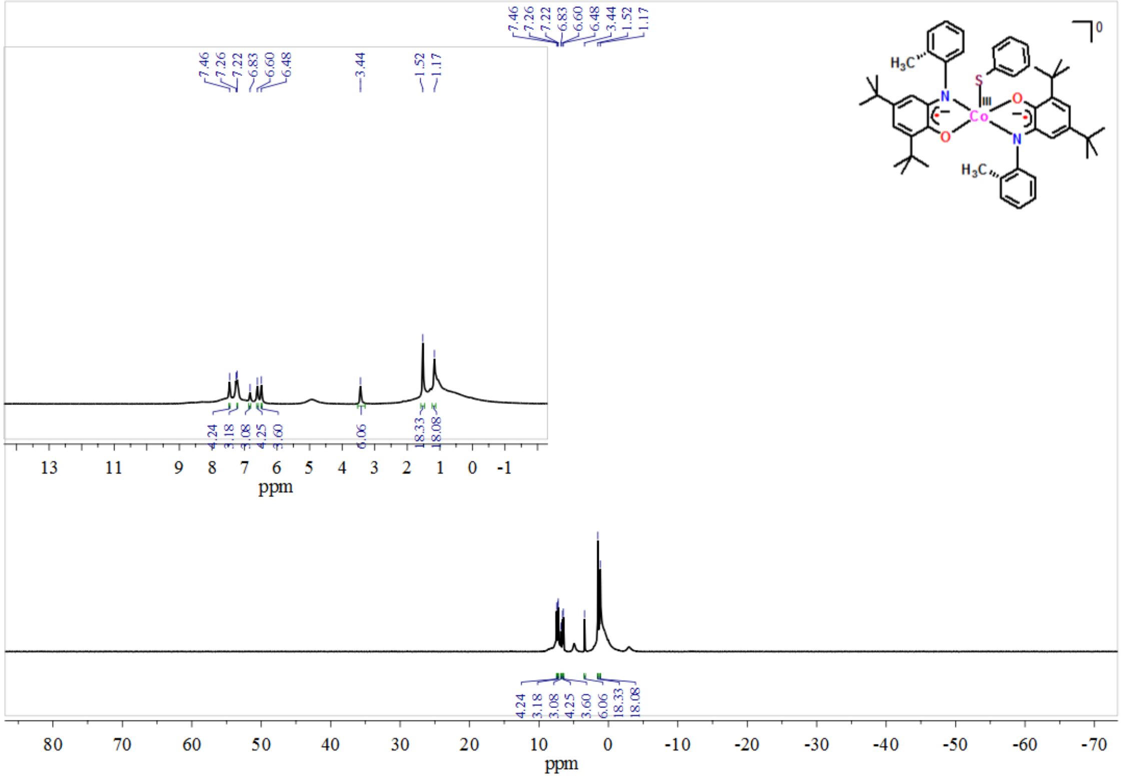

Figure S18. ^{1}H-NMR spectrum of complex **1a** (in $CDCl_3$).

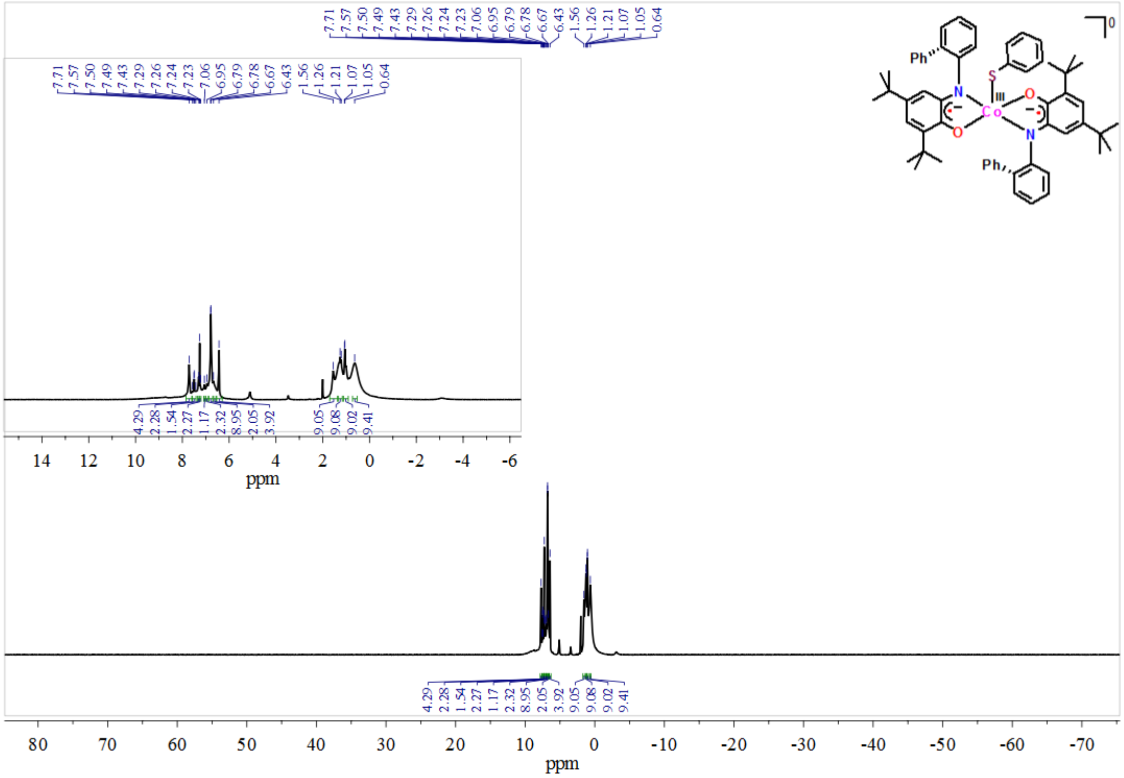

Figure S19. ^{1}H-NMR spectrum of **2a** (in $CDCl_3$).

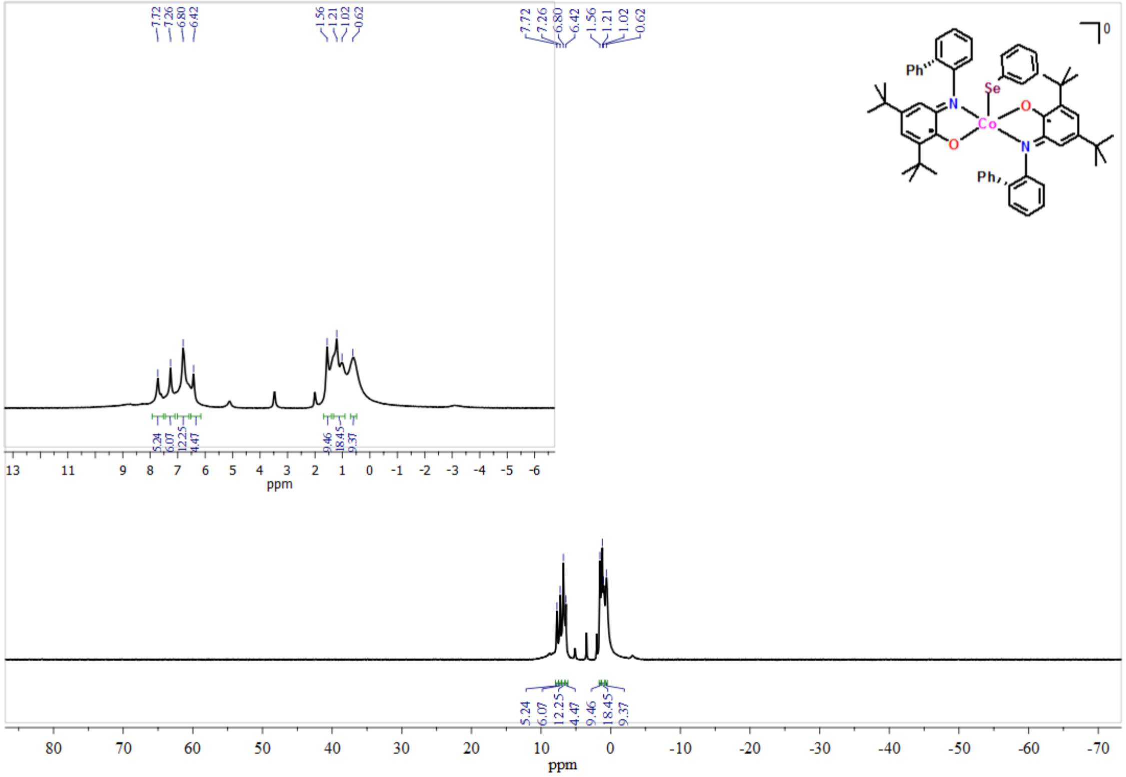

Figure S20. ^{1}H-NMR spectrum of **2b** (in $CDCl_3$).

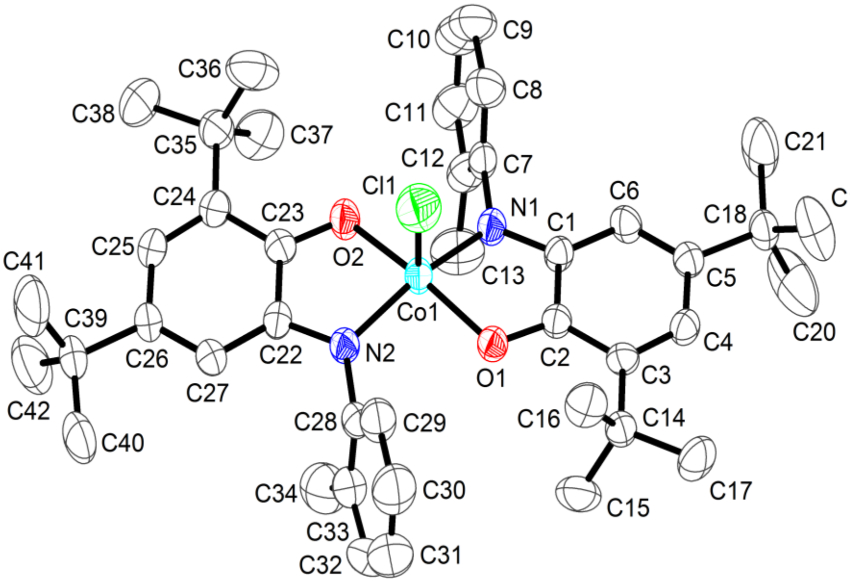

Figure S21. ORTEP diagram of complex **1b**. Hydrogen atoms were omitted for clarity.

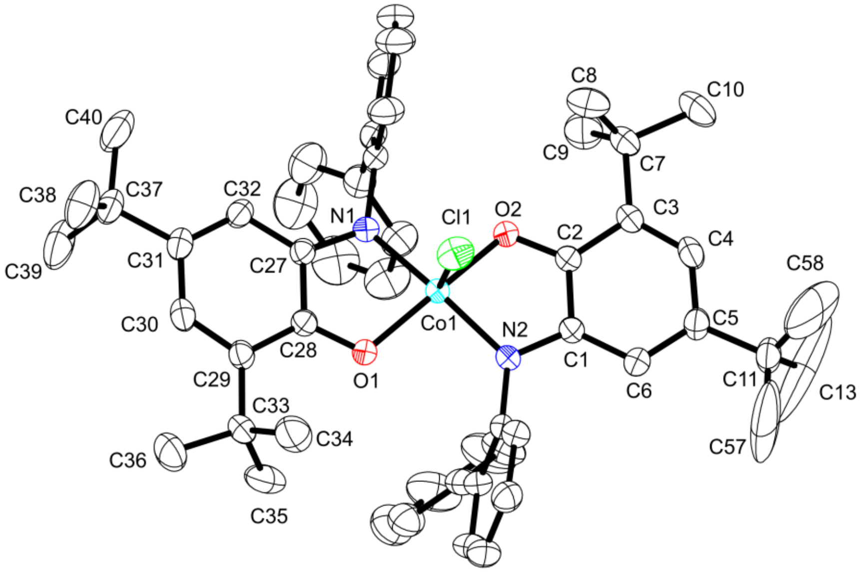

Figure S22. ORTEP diagram of complex **2c**. Hydrogen atoms were omitted for clarity.

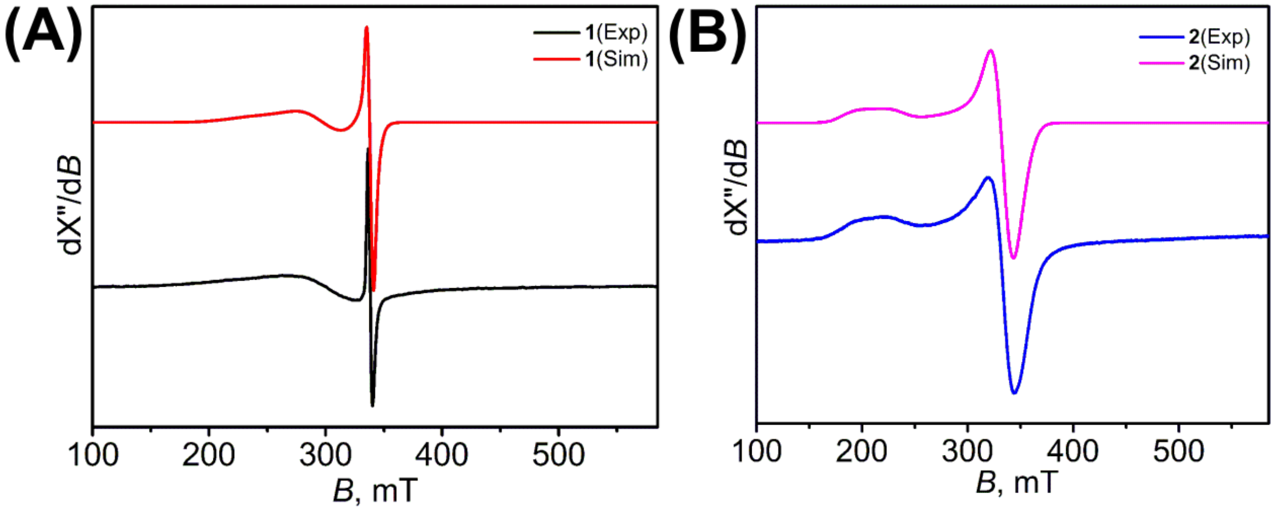

Figure S23. X-band EPR spectra of (A) **1** and (B) **2** in CH_2Cl_2 solution. Conditions: temperature = 25 °C, microwave frequency (GHz) = 9.437[**1**] and 9.442[**2**], modulation frequency (kHz) = 100[**1**and **2**], modulation amplitude (G) = 20.0[**1**] and 50.0[**2**] and microwave power (mW) = 0.998[**1**] and 0.995[**2**].

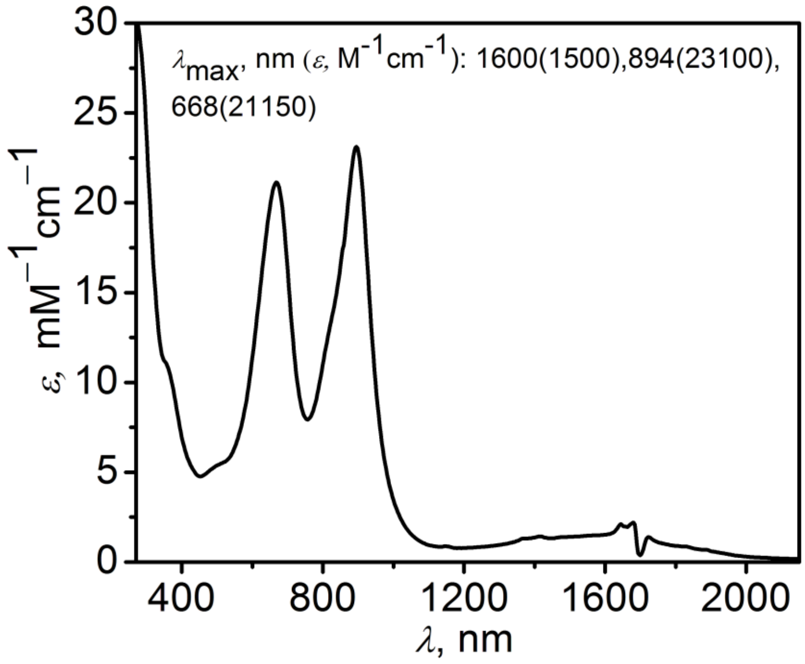

Figure S24. UV-vis/NIR spectrum of complex **1** in CH_2Cl_2 at 25 °C.

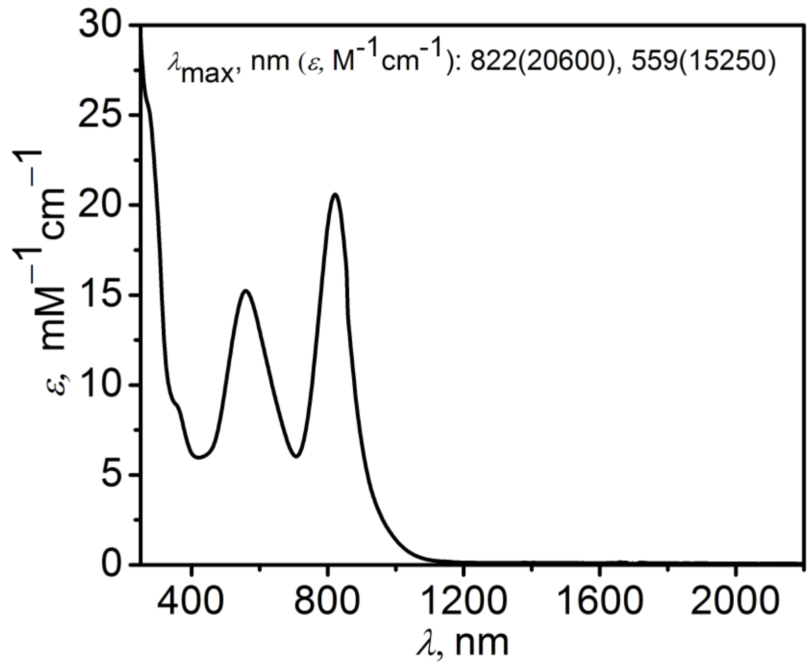

Figure S25. UV-vis/NIR spectrum of complex **1a** in CH_2Cl_2 at 25 °C.

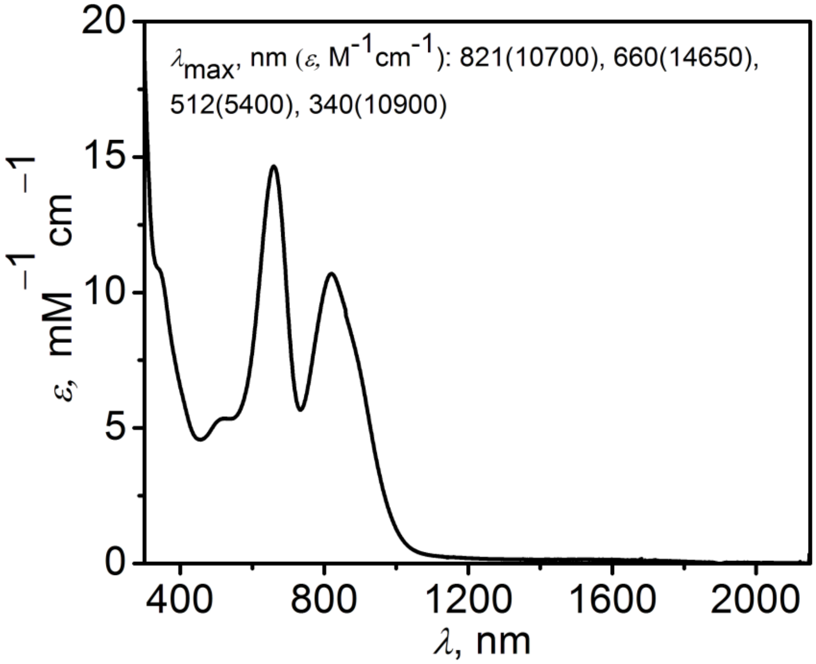

Figure S26. UV-vis/NIR spectrum of complex of **1b** in CH_2Cl_2 at 25 °C.

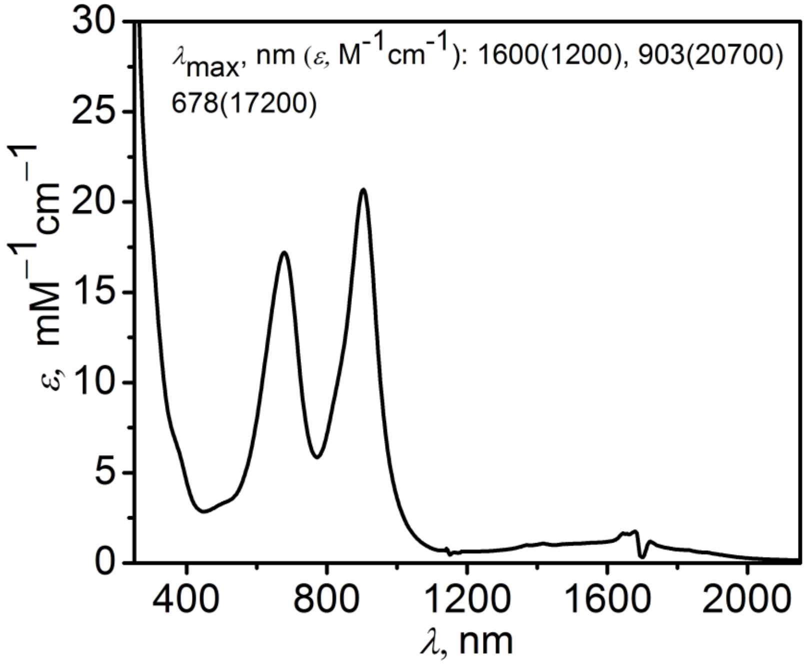

Figure S27. UV-vis/NIR spectrum of complex **2** in CH_2Cl_2 at 25 °C.

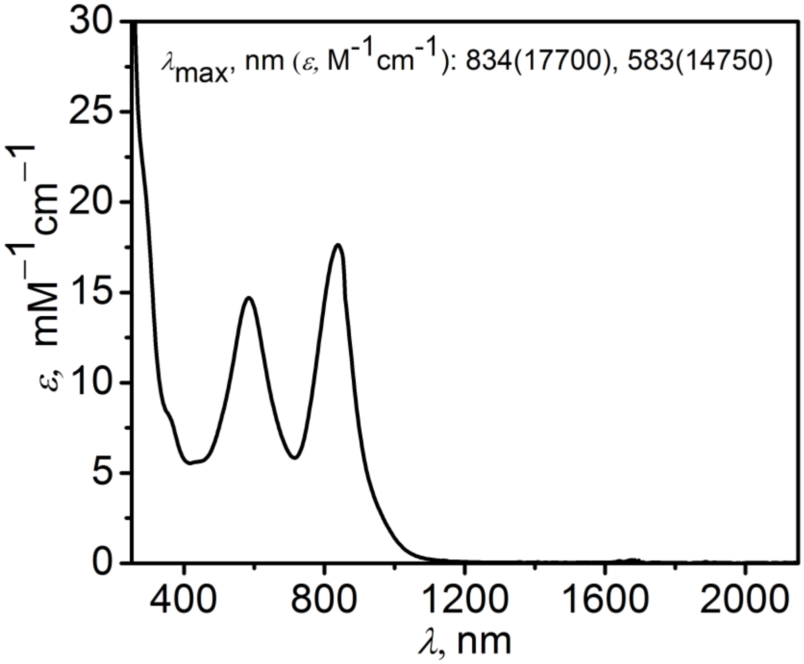

Figure S28. UV-vis/NIR spectrum of complex of **2a** in CH_2Cl_2 at 25 °C.

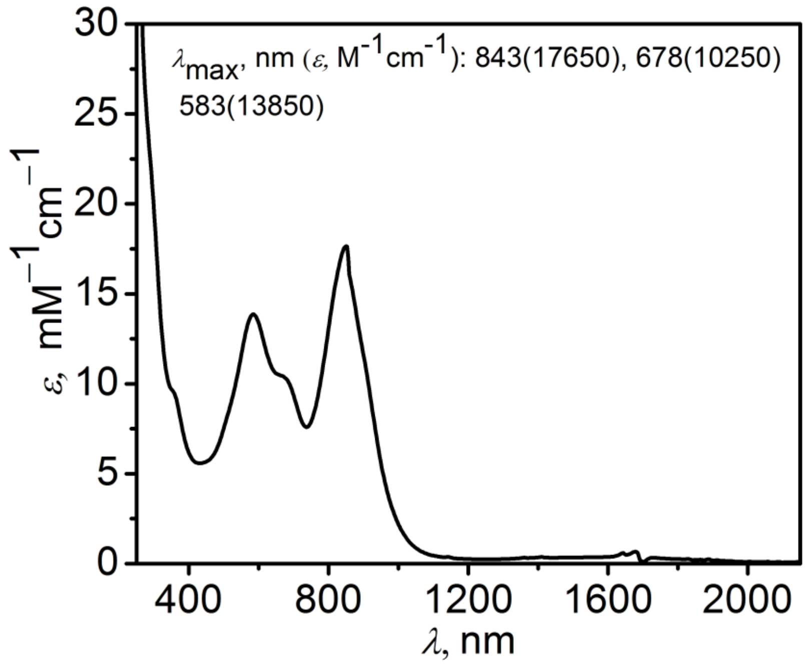

Figure S29. UV-vis/NIR spectrum of complex of complex **2b** in CH_2Cl_2 at 25 °C.

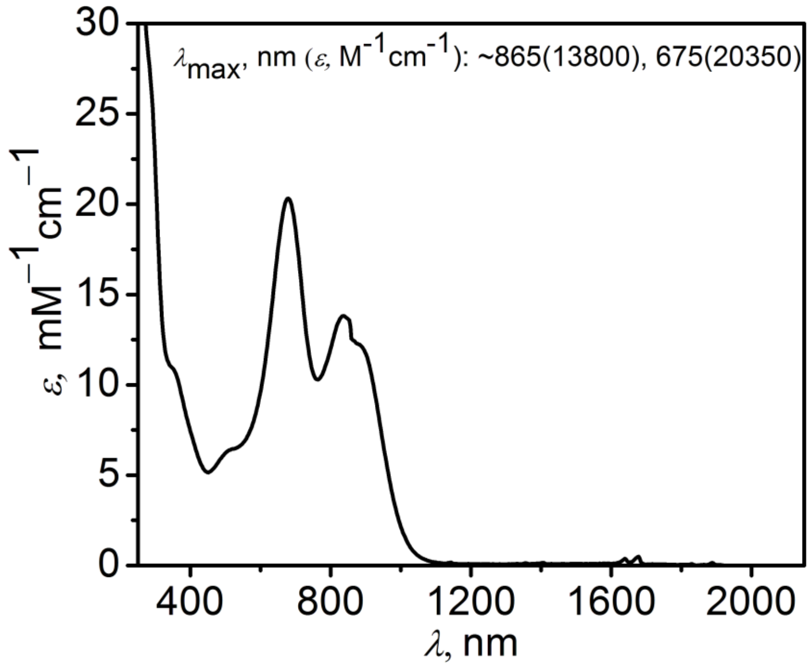

Figure S30. UV-vis/NIR spectrum of complex of complex **2c** in CH_2Cl_2 at 25 °C.

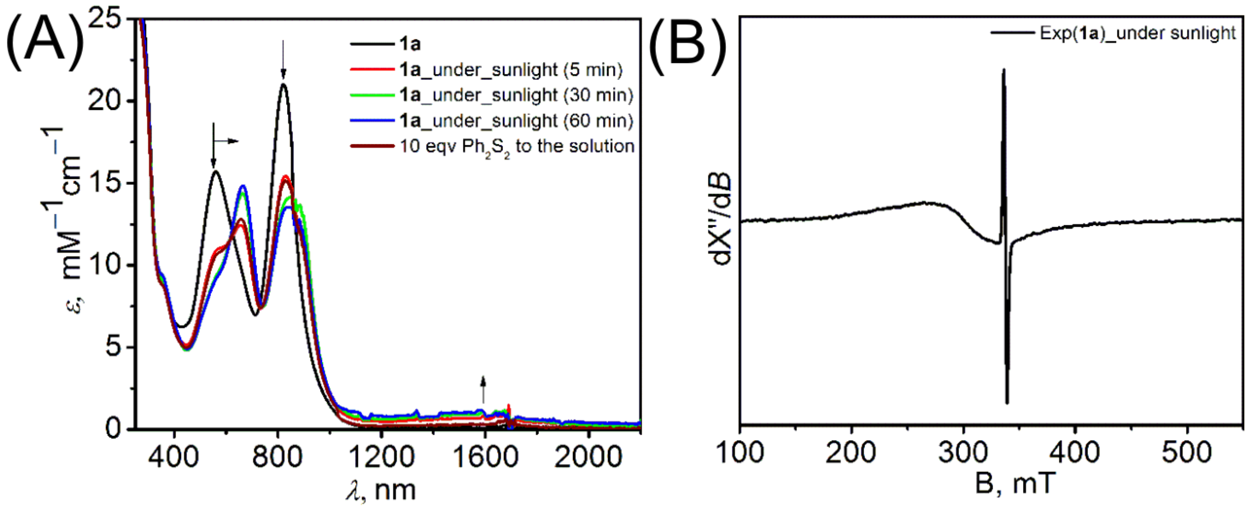

Figure S31. [A] Change in UV-vis/NIR spectrum of **1a** upon exposure to sunlight. Peak shifting towards lower wavelength on addition of Ph_2S_2 into the sunlight-exposed solution emphasized the conversion of four coordinate to five-coordinate complex. [B] Appearance of Co-centered X-band EPR spectrum implied the formation of four-coordinate complex **1** in CH_2Cl_2 solution. Condition: temperature = 25 °C; microwave frequency (GHz) = 9.437; modulation frequency (kHz) = 100; modulation amplitude (G) = 100; and microwave power (mW) = 0.995.

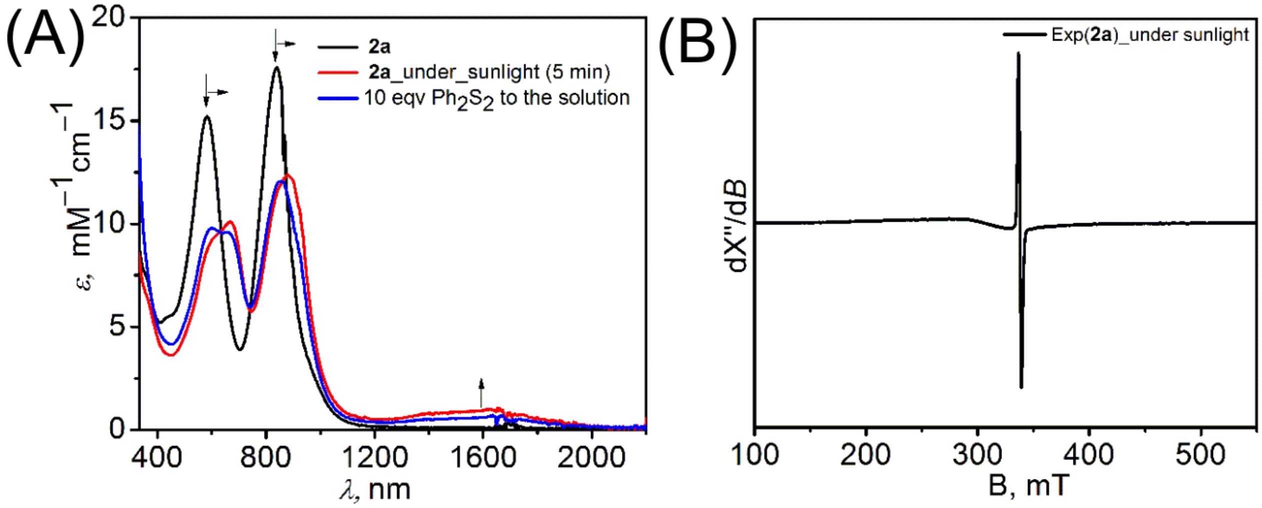

Figure S32. Change in UV-vis/NIR spectrum of **2a** upon exposure to sunlight. Peak shifting towards lower wavelength on addition of Ph_2S_2 into the sunlight-exposed solution emphasized the conversion of four coordinate to five-coordinate complex. [B] Appearance of Co-centered X-band EPR spectrum implied the formation of four-coordinate complex **2** in CH_2Cl_2 solution. Condition: temperature = 25 °C; microwave frequency (GHz) = 9.443; modulation frequency (kHz) = 100; modulation amplitude (G) = 100; and microwave power (mW) = 0.998.

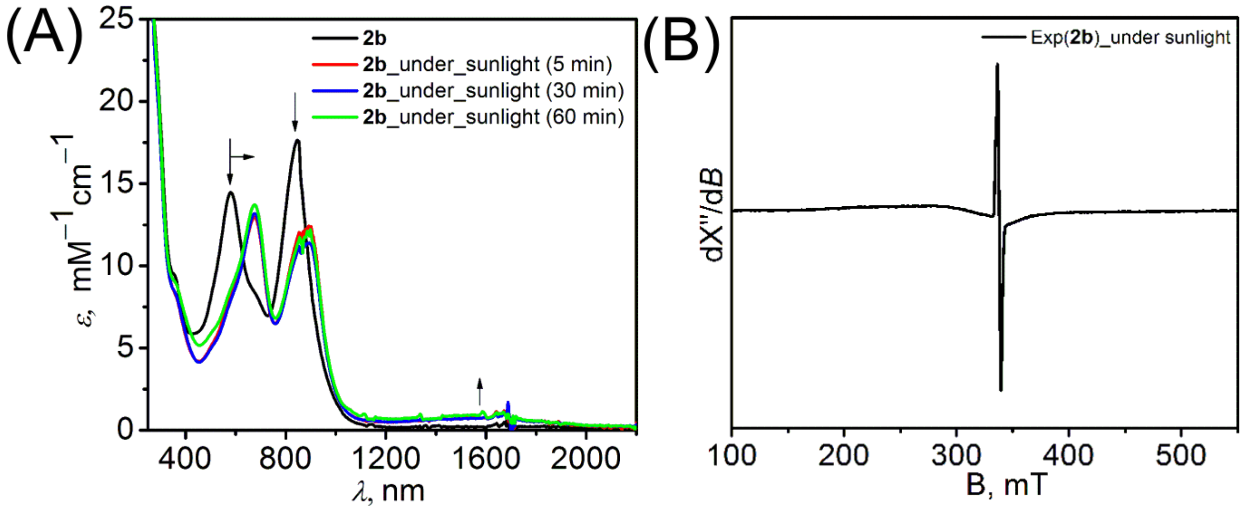

Figure S33. [A] Change in UV-vis/NIR spectrum of **2b** upon exposure to sunlight. [B] Appearance of Co-centered X-band EPR spectrum implied the formation of four-coordinate complex **2** in CH_2Cl_2 solution. Condition: temperature = 25 °C; microwave frequency (GHz) = 9.445; modulation frequency (kHz) = 100; modulation amplitude (G) = 100; and microwave power (mW) = 0.995.

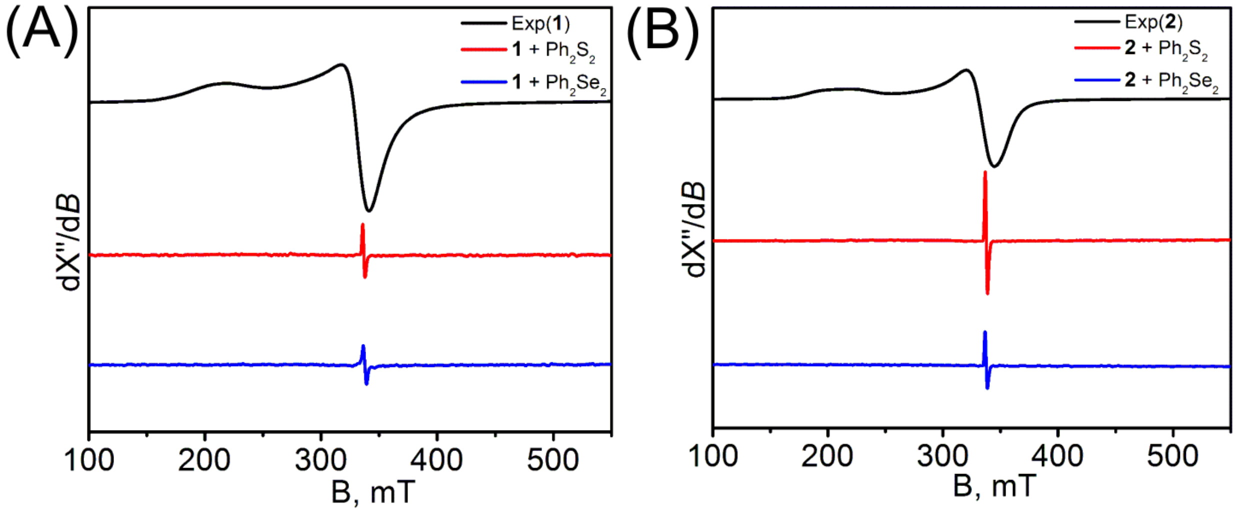

Figure S34. [A] Change in X-band EPR spectrum of **1** with Ph_2S_2 and Ph_2Se_2 in CH_2Cl_2 solution. Conditions: temperature = 25 °C; microwave frequency (GHz) = 9.448[**1**], 9.419[**1**+Ph_2S_2], 9.436[**1**+Ph_2Se_2]; modulation frequency (kHz) = 100[**1**], 100[**1**+Ph_2S_2], 100[**1**+Ph_2Se_2]; modulation amplitude (G) = 10.0[**1**], 70.0[**1**+Ph_2S_2], 70.0[**1**+Ph_2Se_2]; and microwave power (mW) = 0.998[**1**], 0.995[**1**+Ph_2S_2], 0.995[**1**+Ph_2Se_2]. [B] Change in X-band EPR spectrum of **2** with Ph_2S_2 and Ph_2Se_2 in CH_2Cl_2 solution. Condition: temperature = 25 °C; microwave frequency (GHz) = 9.447[**2**], 9.441[**2**+Ph_2S_2], 9.436[**2**+Ph_2Se_2]; modulation frequency (kHz) = 100[**2**], 100[**2**+Ph_2S_2], 100[**2**+Ph_2Se_2]; modulation amplitude (G) = 10.0[**2**], 70.0[**2**+Ph_2S_2], 70.0[**2**+Ph_2Se_2]; and microwave power (mW) = 0.995[**2**], 0.998[**2**+Ph_2S_2], 0.995[**2**+Ph_2Se_2].

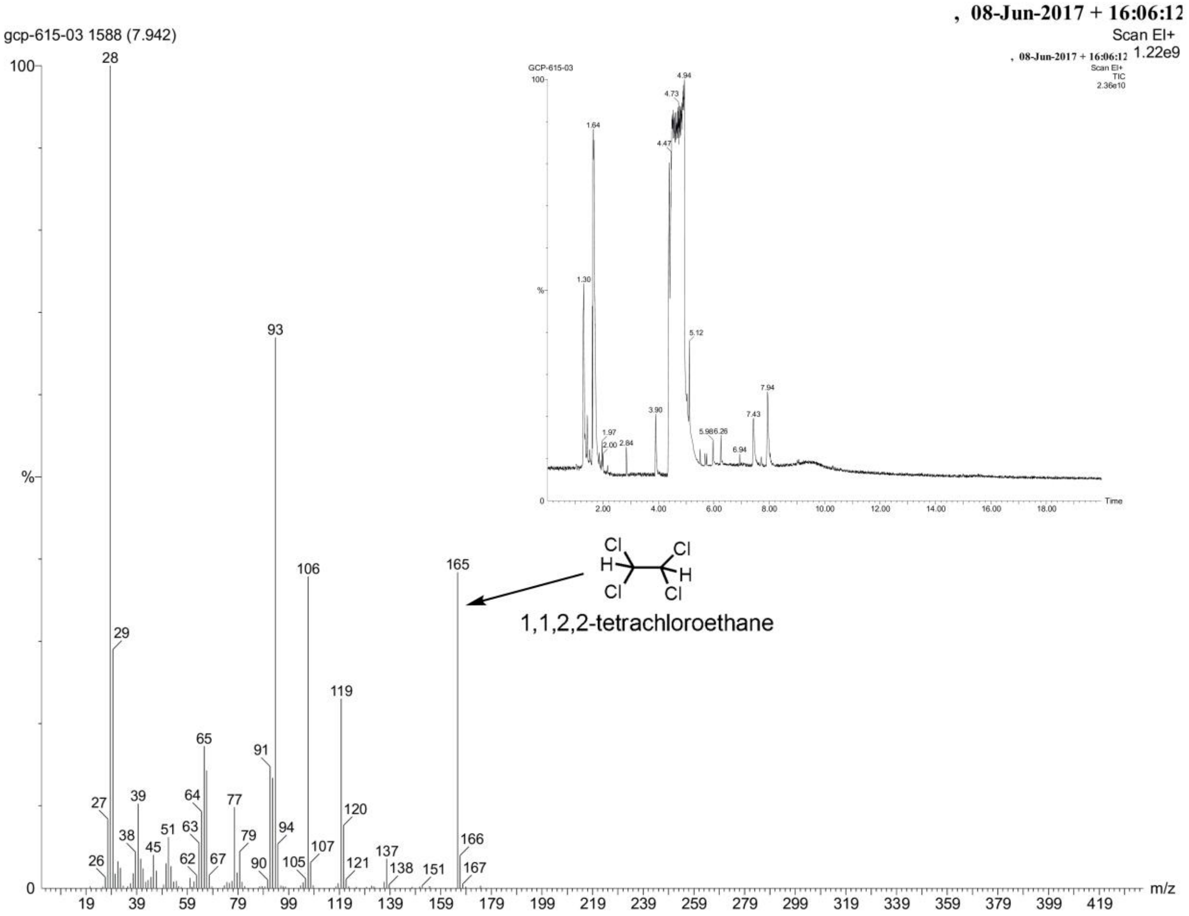

Figure S35. GC-MS spectrum during the catalysis reaction, (inset) chromatogram of the reaction mixture.

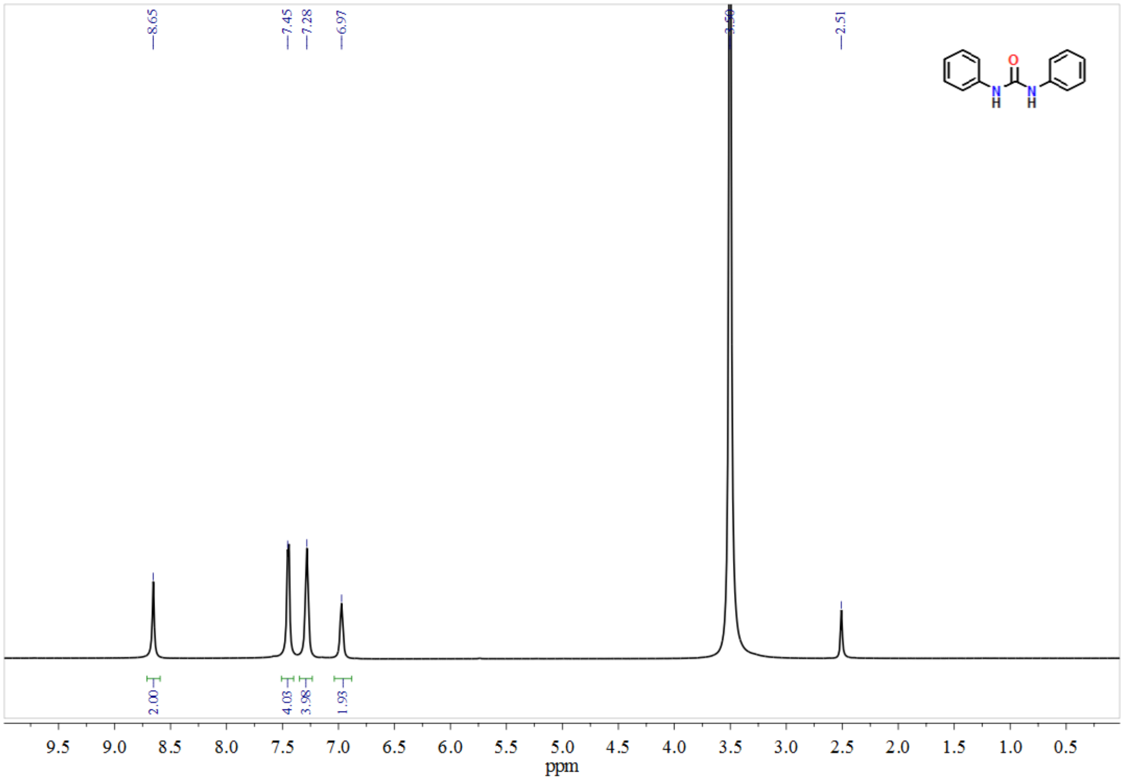

Figure S36. ^{1}H-NMR spectrum of **4a** (in C_2D_6SO solvent).

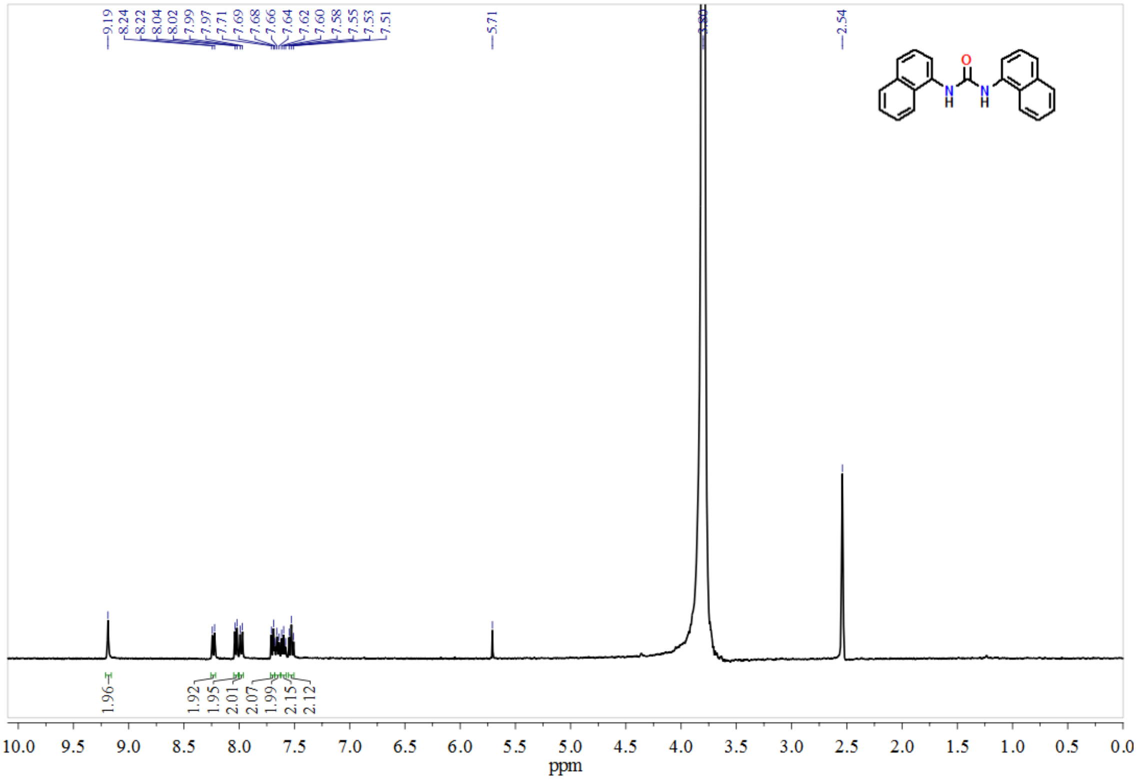

Figure S37. ^{1}H-NMR spectrum of **4b (**in C_2D_6SO solvent).

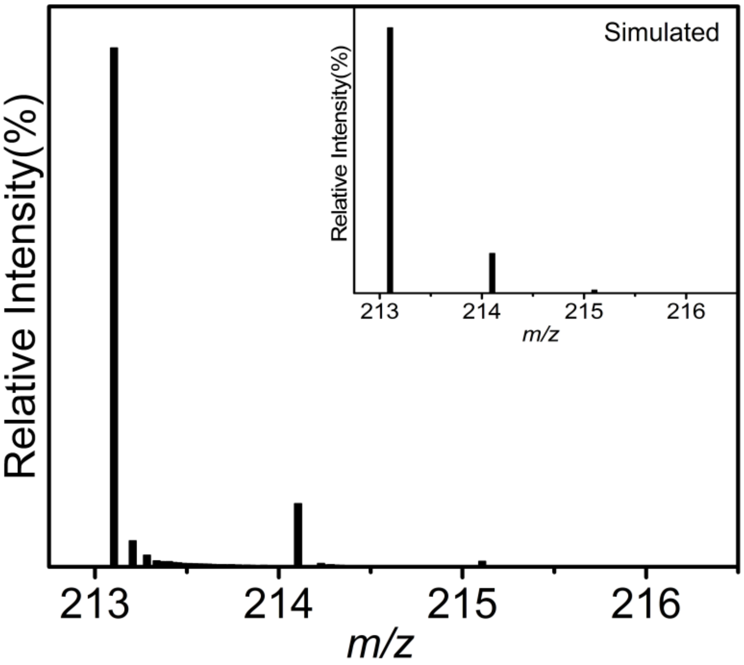

Figure S38. Experimental and simulated mass spectra for **4a** $[C_{13}H_{12}N_2O +H]^+$ have been shown.

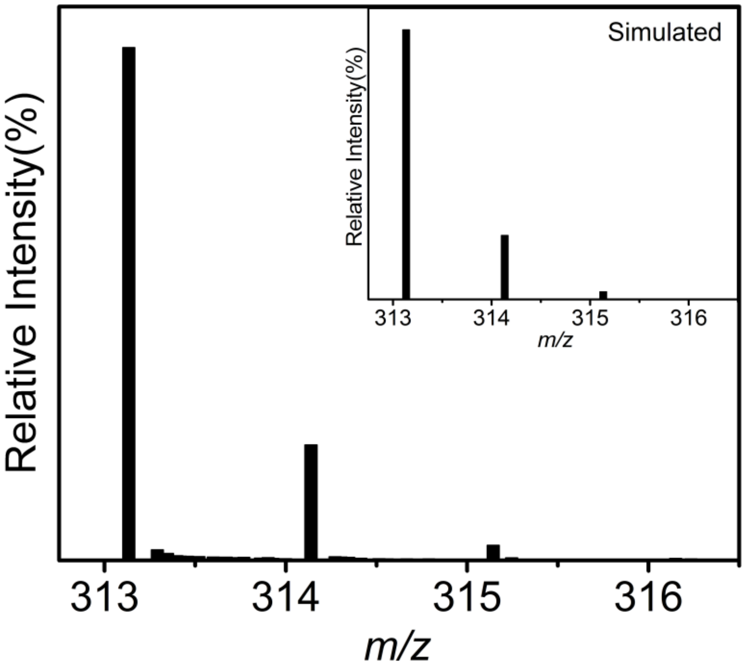

Figure S39. Experimental and simulated mass spectra for **4b** $[C_{21}H_{16}N_2O+H]^+$ have been shown.

Table S2. Selected bond distances (Å) and bond angles (°) of complex **1**.

Co1– O1	1.830(3)	C3– C4	1.386(6)
Co1– N1	1.832(4)	C4– C5	1.415(6)
N1– C1	1.371(5)	C6– C5	1.373(6)
O1– C2	1.323(5)	C6– C1	1.396(6)
C1– C2	1.418(6)	N1– C7	1.437(4)
C3– C2	1.412(6)		
N1– Co1– N1^{i}	180.000(2)	O1– Co1– O1^{i}	180.0(2)
O1– Co1– N1	85.62(14)	C1– N1– Co1	113.9(3)
O1– Co1– N1^{i}	94.38(14)	C7– N1– Co1	126.3(3)
C1– C2– O1	115.5(4)	C2– O1– Co1	113.6(3)

Table S3. Selected bond distances (Å) and bond angles (°) of complex **1a**.

Co1– N1	1.853(3)	C4– C5	1.430(5)
Co1– N2	1.859(3)	C5– C6	1.368(5)
Co1– O1	1.861(2)	C6– C1	1.422(5)
Co1– O2	1.858(2)	N1– C7	1.437(5)
Co1– S1	2.2859(14)	C22– C23	1.427(5)
N1– C1	1.346(4)	C23– C24	1.435(5)
N2– C22	1.353(5)	C24– C25	1.385(5)
O1– C2	1.312(4)	C25– C26	1.428(5)
O2– C23	1.310(4)	C26– C27	1.357(5)
C1– C2	1.421(5)	C27– C22	1.418(5)
C2– C3	1.429(5)	N2– C28	1.437(5)
C3– C4	1.376(5)		
N1– Co1– N2	163.88(14)	C43–S1–Co1	108.07(16)
O1– Co1– O2	166.81(12)	C23–O2–Co1	113.9(2)
O1– Co1– N1	83.95(12)	C2–O1–Co1	114.1(2)
O2– Co1– N2	84.02(12)	C1–N1–Co1	114.4(2)
N1– Co1– O2	93.65(12)	C7–N1–Co1	125.3(2)
N2– Co1– O1	94.68(12)	C1–N1–C7	119.5(3)
N2– Co1– S1	99.83(11)	C22–N2–Co1	114.3(2)
N1– Co1– S1	96.28(10)	C28–N2–Co1	125.7(2)
O2– Co1– S1	100.85(9)	C22–N2–C28	120.0(3)
O1– Co1– S1	92.31(9)		

Table S4. Selected bond distances (Å) and bond angles (°) of complex **1b**.

Co1– N1	1.852(3)	C3– C4	1.370(5)
Co1– N2	1.858(3)	C4– C5	1.437(5)
Co1– O1	1.872(2)	C5– C6	1.350(5)
Co1– O2	1.868(2)	C6– C1	1.414(4)
Co1– Cl1	2.2753(15)	N1– C7	1.436(4)
N1– C1	1.345(4)	C22– C23	1.432(5)
O1– C2	1.291(4)	C23– C24	1.425(5)
N2– C22	1.352(4)	C24– C25	1.370(5)
O2– C23	1.295(4)	C25– C26	1.439(5)
C1– C2	1.446(4)	C26– C27	1.357(5)
C2– C3	1.434(4)	C27– C22	1.405(5)
N1– Co1– N2	158.11(17)	O2– Co1– Cl1	96.40(11)
O1– Co1– N2	94.35(11)	N1–Co1–Cl1	101.65(13)
N2– Co1– O2	83.50(11)	C23– O2–Co1	114.2(2)
O1– Co1–N1	83.60(10)	C2– O1–Co1	113.9(2)
O1– Co1– O2	167.75(14)	C1– N1– Co1	115.0(2)
O2– Co1–N1	93.89(11)	C7– N1–Co1	125.4(2)
O1– Co1–Cl1	95.85(10)	C22– N2–Co1	114.6(2)
N2– Co1–Cl1	100.24(12)	C28– N2– Co1	123.8(2)

Table S5. Selected bond distances (Å) and bond angles (°) of complex **2a**.

Co1– N1	1.858(2)	C4–C5	1.433(4)
Co1– N2	1.850(2)	C5–C6	1.363(4)
Co1– O1	1.8562(19)	C6–C1	1.412(4)
Co1– O2	1.8713(19)	C28–C27	1.430(4)
Co1– S1	2.2822(9)	C28–C29	1.421(4)
Co2– N3	1.856(2)	C29–C30	1.381(4)
Co2– N4	1.863(2)	C30–C31	1.421(4)
Co2– O3	1.857(2)	C32–C31	1.357(4)
Co2– O4	1.856(2)	C27–C32	1.409(4)
Co2– S2	2.2731(11)	C59–C60	1.437(4)
O1– C2	1.307(3)	C60–C61	1.428(4)
O2– C28	1.306(3)	C61–C62	1.370(4)
N1– C1	1.352(3)	C62–C63	1.428(4)
N2– C27	1.351(4)	C63–C64	1.363(4)
N3–C59	1.350(4)	C64–C59	1.415(4)
N4–C85	1.354(4)	C85–C86	1.430(4)
O3– C60	1.304(3)	C86–C87	1.430(4)
O4– C86	1.302(4)	C87–C88	1.371(5)
C1– C2	1.428(4)	C88–C89	1.431(5)
C2– C3	1.424(4)	C89–C90	1.358(5)
C3–C4	1.367(4)	C85–C90	1.417(4)

N2–Co1–O1	93.05(9)	N1–Co1–S1	99.15(8)
N2–Co1–N1	162.91(11)	O2–Co1–S1	90.96(7)
O1–Co1–N1	84.02(9)	N1–Co1–O2	95.20(9)
N2–Co1–O2	84.24(9)	N2–Co1–S1	97.94(8)
O1–Co1–O2	168.20(9)	O1–Co1–S1	100.80(7)
O4–Co2–N3	93.56(10)	O4–Co2–N3	93.56(10)
O4–Co2–O3	168.37(10)	O4–Co2–S2	88.61(8)
N3–Co2–O3	84.06(10)	N3–Co2–S2	99.65(9)
O4–Co2–N4	84.26(10)	O3–Co2–S2	103.00(7)
N3–Co2–N4	163.08(12)	N4–Co2–S2	97.07(9)

Table S6. Selected bond distances (Å) and bond angles (°) of complex **2b** at 100 K.

Co1– N1	1.845(5)	C4–C5	1.438(11)
Co1– N2	1.856(5)	C6–C5	1.355(11)
Co1– O1	1.856(5)	C6–C1	1.425(10)
Co1– O2	1.881(5)	C27–C28	1.426(10)
Co1– Se1	2.4007(12)	C28–C29	1.461(10)
Co2– N3	1.871(6)	C29–C30	1.357(10)
Co2– N4	1.855(6)	C30–C31	1.416(11)
Co2– O3	1.840(5)	C31–C32	1.412(11)
Co2– O4	1.842(5)	C27–C32	1.415(10)
Co2– Se2	2.3965(12)	C59–C60	1.423(10)
O1– C2	1.307(8)	C60–C61	1.418(10)
O2– C28	1.289(8)	C61–C62	1.385(11)
N1– C1	1.380(9)	C62–C63	1.428(10)
N2– C27	1.343(9)	C63–C64	1.371(11)
N3–C59	1.339(9)	C64–C59	1.420(10)
N4–C85	1.365(9)	C85–C86	1.441(9)
O3– C60	1.310(8)	C86–C87	1.439(10)
O4– C86	1.309(8)	C87–C88	1.349(10)
C1– C2	1.422(9)	C88–C89	1.439(11)
C2– C3	1.412(11)	C89–C90	1.330(10)
C3–C4	1.380(11)	C85–C90	1.413(10)
N2– Co1– O1	93.6(2)	N1– Co1– O2	93.2(2)
N2– Co1– N1	162.5(3)	O2– Co1– Se1	98.20(16)
O1– Co1– N1	84.0(2)	N2– Co1– Se1	100.55(18)
N2– Co1– O2	83.8(2)	O1– Co1– Se1	99.33(16)
O1– Co1– O2	162.5(2)	N1– Co1– Se1	96.93(18)
O4– Co2– N3	94.2(2)	O4–Co2–N3	163.8(3)
O4– Co2– O3	163.5(2)	O4–Co2–Se2	97.56(16)
N3– Co2– O3	83.4(2)	N3–Co2–Se2	96.2(2)
O4– Co2– N4	84.7(2)	O3–Co2–Se2	98.88(16)
N3– Co2– N4	163.8(3)	N4–Co2–Se2	100.00(18)

Table S7. Selected bond distances (Å) and bond angles (°) of complex **2c**.

Co1– N1	1.873(2)	C3– C4	1.370(4)
Co1– N2	1.865(2)	C4– C5	1.430(4)
Co1– O1	1.8553(18)	C5– C6	1.368(4)
Co1– O2	1.8694(19)	C6– C1	1.417(4)
Co1– Cl1	2.2661(9)	N1– C15	1.442(3)
N1– C1	1.341(3)	C27– C28	1.443(4)
O1– C2	1.300(3)	C28– C29	1.433(4)
N2– C27	1.337(3)	C29– C30	1.368(4)
O2– C28	1.291(3)	C30– C31	1.446(4)
C1– C2	1.434(4)	C31– C32	1.358(4)
C2– C3	1.425(4)	C32– C27	1.416(4)
N1– Co1– N2	167.33(10)	O2– Co1– Cl1	97.78(7)
O1– Co1– N2	93.64(9)	N1–Co1–Cl1	95.32(7)
N2– Co1– O2	83.70(9)	C28– O2–Co1	113.67(17)
O1– Co1–N1	83.94(9)	C2– O1–Co1	112.84(17)
O1– Co1– O2	168.71(9)	C1– N1– Co1	112.62(18)
O2– Co1–N1	96.25(9)	C15– N1–Co1	124.89(17)
O1– Co1–Cl1	93.43(7)	C27– N2–Co1	114.09(18)
N2– Co1–Cl1	97.23(7)	C41– N2– Co1	124.95(18)

Table S8. Crystallographic parameters and refinement data for complex **1**.

Name	Complex **1**
Empirical formula	$C_{42} H_{52}CoN_2O_2$
Formula weight	675.79
CCDC Number	1454093
Crystal habit, colour	Block, Green
Crystal size, mm^3	0.32×0.24×0.20
Temperature, T	293(2)
Wavelength, λ (Å)	0.71073
Crystal system	Triclinic
Space group	'P –1'
Unit cell dimensions	a = 5.9742(3) Å b = 12.7038(11) Å c = 13.2139(7) Å α = 73.037(7)°, β = 85.630(4)°, γ = 83.989(7)°
Volume, V (Å^3)	952.87(11)
Z	1
Calculated density, $Mg \cdot m^{-3}$	1.178
Absorption coefficient, μ (mm^{-1})	0.486
F(000)	361
θ range for data collection	3.18° to 25.00°
Limiting indices	$-5 \leq h \leq 7$, $-15 \leq k \leq 15$, $-15 \leq l \leq 15$
Reflection collected/unique	6518/ 3319 [R(int)= 0.0203]
Completeness to θ	99.1% (θ = 25.00°)
Max. and min. transmission	0.907/ 0.869
Refinement method	'SHELXL–97(Sheldrick, 1997)'
Data/restraints/parameters	3319 /0/ 219
Goodness–of–fit on F^2	1.053
Final R indices [I>2σ(I)]	$R1$ = 0.0783, $wR2$ = 0.2027
R indices (all data)	$R1$ = 0.0993, $wR2$ = 0.2212
Largest diff. peak and hole	0.735 and –0.547 $e \cdot Å^{-3}$

Table S9. Crystallographic parameters and refinement data for complex **1a**.

Name	Complex **1a**
Empirical formula	$C_{48}H_{59}CoN_2O_2S$
Formula weight	786.96
CCDC Number	1547976
Crystal habit, colour	Block, Blue
Crystal size, mm^3	0.52×0.42×0.30
Temperature, T	293(2)
Wavelength, λ (Å)	0.71073
Crystal system	Triclinic
Space group	'P –1'
Unit cell dimensions	a = 12.6348(9) Å b = 14.2874(18) Å c = 14.4663(10) Å α = 99.892(6)°, β = 113.792(4)°, γ = 102.214(6)°
Volume, V ($Å^3$)	2236.8(4)
Z	2
Calculated density, $Mg \cdot m^{-3}$	1.168
Absorption coefficient, μ (mm^{-1})	0.468
F(000)	840
θ range for data collection	1.82° to 24.50 °
Limiting indices	$-14 \leq h \leq 14$, $-16 \leq k \leq 16$, $-16 \leq l \leq 16$
Reflection collected/unique	27091/ 7088 [R(int)= 0.0618]
Completeness to θ	95.1% (θ = 24.50°)
Max. and min. transmission	0.869/ 0.790
Refinement method	'SHELXL–97(Sheldrick, 1997)'
Data/restraints/parameters	7088 /0/ 501
Goodness–of–fit on F^2	1.022
Final R indices [$I > 2\sigma(I)$]	$R1$ = 0.0550, $wR2$ = 0.1227
R indices (all data)	$R1$ = 0.1238, $wR2$ = 0.1634
Largest diff. peak and hole	0.494 and – 0.456 $e \cdot Å^{-3}$

Table S10. Crystallographic parameters and refinement data for complex **1b**.

Name	Complex **1b**
Empirical formula	$C_{42}H_{54}ClCoN_2O_2$
Formula weight	713.25
CCDC Number	1555498
Crystal habit, colour	Block, Blue
Crystal size, mm^3	0.36×0.30×0.28
Temperature, T	293(2)
Wavelength, λ (Å)	0.71073
Crystal system	Tetragonal
Space group	' P 43'
Unit cell dimensions	a = 15.3395(2) Å b = 15.3395(2) Å c = 16.7305(6) Å $\alpha = \beta = \gamma = 90.00°$
Volume, V ($Å^3$)	3936.69(16)
Z	4
Calculated density, $Mg \cdot m^{-3}$	1.203
Absorption coefficient, μ (mm^{-1})	0.539
F(000)	1520
θ range for data collection	2.92 ° to 24.99°
Limiting indices	$-18 \leq h \leq 14$, $-17 \leq k \leq 18$, $-19 \leq l \leq 19$
Reflection collected/unique	8776 / 5755 [R(int)= 0.0241]
Completeness to θ	99.8 % (θ = 24.99°)
Max. and min. transmission	0.860/0.824
Refinement method	'SHELXL–97(Sheldrick, 1997)'
Data/restraints/parameters	5755 / 0 / 447
Goodness–of–fit on F^2	1.043
Final R indices [$I>2\sigma(I)$]	$R1$ = 0.0448, $wR2$ = 0.1046
R indices (all data)	$R1$ = 0.0542, $wR2$ = 0.1135
Largest diff. peak and hole	0.239 and –0.253 $e \cdot Å^{-3}$

Table S11. Crystallographic parameters and refinement data for complex **2a**.

Complex	Complex **2a**
Empirical formula	$C_{58}H_{63}CoN_2O_2S$
Formula weight	910.39
CCDC Number	1547977
Crystal habit, colour	Needle, Dark Blue
Crystal size, mm^3	0.20×0.15×0.10
Temperature, *T*	293(2)
Wavelength, λ (Å)	0.71073
Crystal system	Monoclinic
Space group	'*P* 21/n'
Unit cell dimensions	a = 13.2465(3) Å b = 16.1975(4) Å c = 48.3989(8) Å $\alpha = 90.00°$, $\beta = 92.1863(17)°$, $\gamma = 90.00°$
Volume, V (Å^3)	10376.9(4)
Z	8
Calculated density, Mg·m^{-3}	1.166
Absorption coefficient, μ (mm^{-1})	0.413
F(000)	3872
θ range for data collection	3.03° to 25.00°
Limiting indices	$-15 \leq h \leq 15$, $-19 \leq k \leq 15$, $-57 \leq l \leq 41$
Reflection collected/unique	48525/18243 [*R*(int)= 0.0363]
Completeness to θ	99.8% ($\theta = 25.00°$)
Max. and min. transmission	0.978/0.960
Refinement method	'SHELXL–97(Sheldrick, 1997)'
Data/restraints/parameters	18243 /0/1177
Goodness–of–fit on F^2	1.076
Final *R* indices [$I>2\sigma(I)$]	$R1 = 0.0581$, $wR2 = 0.1260$
R indices (all data)	$R1 = 0.0764$, $wR2 = 0.1358$
Largest diff. peak and hole	0.498 and – 0.332e·Å^{-3}

Table S12. Crystallographic parameters and refinement data for complex **2b** (at 100 K).

Name	Complex **2b**
Empirical formula	$C_{116}H_{127}Co_2N_4O_4Se_2$
Formula weight	1917.00
CCDC Number	1547978
Crystal habit, colour	Needle, Blue
Crystal size, mm^3	0.26×0.17×0.12
Temperature, T	100(2)
Wavelength, λ (Å)	0.71073
Crystal system	Monoclinic
Space group	'P 21'
Unit cell dimensions	a = 10.5924(5) Å b = 36.8212(15) Å c = 14.0563(6) Å α = 90.00°, β = 96.839(4)°, γ = 90.00°
Volume, V (Å^3)	5443.3(4)
Z	2
Calculated density, $Mg\cdot m^{-3}$	1.170
Absorption coefficient, μ (mm^{-1})	1.024
$F(000)$	2010
θ range for data collection	3.13° to 25.00°
Limiting indices	$-12 \leq h \leq 8$, $-43 \leq k \leq 41$, $-15 \leq l \leq 16$
Reflection collected/unique	26610/17459 [R(int)= 0.0313]
Completeness to θ	99.1% (θ = 25.00°)
Max. and min. transmission	0.884/0.811
Refinement method	'SHELXL–97(Sheldrick, 1997)'
Data/restraints/parameters	17459 /1/1178
Goodness–of–fit on F^2	1.076
Final R indices [$I>2\sigma(I)$]	$R1 = 0.0704$, $wR2 = 0.1630$
R indices (all data)	$R1 = 0.0910$, $wR2 = 0.1804$
Largest diff. peak and hole	0.989 and –0.492 e·Å^{-3}

Table S13. Crystallographic parameters and refinement data for complex **2c**.

Name	Complex **2c**
Empirical formula	C_{52} $H_{58}ClCoN_2O_2$, CH_3CN
Formula weight	878.44
CCDC Number	1547979
Crystal habit, colour	Needle, Blue
Crystal size, mm^3	0.24×0.18×0.14
Temperature, T	293(2)
Wavelength, λ (Å)	0.71073
Crystal system	Triclinic
Space group	'P –1'
Unit cell dimensions	a = 12.6286(6) Å b = 14.1944(5) Å c = 15.1025(5) Å α = 79.358(3) °, β = 78.791(3) °, γ = 68.866(4) °
Volume, V ($Å^3$)	2457.45(17)
Z	2
Calculated density, $Mg\cdot m^{-3}$	1.187
Absorption coefficient, μ (mm^{-1})	0.445
$F(000)$	932
θ range for data collection	3.00° to 25.00°
Limiting indices	$-14 \leq h \leq 15$, $-16 \leq k \leq 14$, $-17 \leq l \leq 17$
Reflection collected/unique	18632 / 8628 [R(int)= 0.0244]
Completeness to θ	99.8% (θ = 25.00°)
Max. and min. transmission	0.940 / 0.908
Refinement method	'SHELXL–97(Sheldrick, 1997)'
Data/restraints/parameters	8628 /0/ 563
Goodness–of–fit on F^2	1.032
Final R indices [$I>2\sigma(I)$]	$R1 = 0.0547$, $wR2 = 0.1385$
R indices (all data)	$R1 = 0.0694$, $wR2 = 0.1522$
Largest diff. peak and hole	0.828and –0.599 $e\cdot Å^{-3}$

References:

1. X. Wang, G. Liu, X. H. Xu, N. Shibata, E. Tokunaga and N. Shibata, *Angew. Chem. Int. Ed*. 2014, **53**, 1827.

2. CrysAlisPro, Oxford Diffraction Ltd., Version 1, 171. 33. 34d [release 27-02-2009 CrysAlis 171. NET];

3. G. M. Sheldrick, Acta Crystallogr. 2008, **A64**, 112.

4. S. Ghorai and C. Mukherjee, *Chem. Commun.*, 2012, **48**, 10180.